Latin American Journal of Solids and Structures
www.lajss.org

# Novel Layerwise Shear Correction Factors for Zigzag Theories of Circular Sandwich Plates with Functionally Graded Layers

**Abstract**

The available shear correction factors have mainly been proposed for single-layer rectangular plates with zero shear tractions and isotropic homogenous materials. The present analytical shear factors are especially suitable for the first-order zigzag or layerwise theories of circular sandwich plates with functionally graded cores/face sheets and simultaneous normal and shear tractions. Although the present layerwise correction factors are general, they are evaluated for the modal analyses where effects of the shear correction are more remarkable than those of the stress analyses. It is the first time that the concept of the local shear correction factor is introduced. To present more accurate results, the Mori-Tanaka micromechanical-based material properties model is used instead of the traditional rule of mixtures. The governing equations are solved using the analytical Taylor transform method. Comparisons made among results associated with the known shear correction factors, present results, and results of the three-dimensional theory of elasticity reveal that significant enhancements may occur through using the proposed analytical shear correction factors.

**Keywords**

Local shear correction factors; analytical Taylor transform solution; functionally graded circular sandwich plate; zigzag theory; free vibration.

**M. Shariyat** [a]
**M.M. Alipour** [b]

[a] Professor, Faculty of Mechanical Engineering, K.N. Toosi University of Technology, Tehran, Iran.
Email: m_shariyat@yahoo.com
(Corresponding author)
[b] Ph.D., Faculty of Mechanical Engineering, K.N. Toosi University of Technology, Tehran, Iran.
Email: m.mollaalipur@gmail.com

http://dx.doi.org/10.1590/1679-78251477

Received 23.07.2014
Accepted 21.10.2015
Available online 11.11.2014

## 1 INTRODUCTION

Three-layer sandwich plates with protective or load carrying face sheets and spacer, damper, or stiffener cores have extensively been employed in various engineering applications and hi-tech structures. Various requirements may be covered through using different combinations of the stiff or soft materials for the face sheets and cores. Employing functionally graded face sheets or cores may reduce or eliminate the discontinuities in the distribution of the transverse stresses at the interfaces between the layers.

Although the three-dimensional theory of elasticity is an accurate approach this theory cannot be directly applied with ease for multilayer plates with arbitrary variations of the material properties, non-uniform tractions, and general geometries and boundary conditions, especially when thickness of the layers is small. Majority of the researchers have used equivalent single layer theories (Reddy, 2005; Shariyat, 2009a; Shariyat, 2009b; Ebrahimi et al., 2009; Mantari and Oktem, 2011; Sofiyev, 2014) for analysis of the multilayer plates. It is evident that accuracy of these theories may encounter problems when number of the layers increases or when the material properties experience severe changes in the transverse direction. In such cases, using the layerwise or zigzag theories is more appropriate (Pandit et al., 2008; Fares and Elmarghany, 2008; Shariyat, 2010; Shariyat, 2012a). For the both general categories of the plates, i.e., the equivalent single-layer and zigzag first-order theories, the first-order shear-deformation theories (FSDT) are computationally more economic and relatively simpler. For these reasons, they have been attractive for performing the stress and bending (Alipour, and Shariyat, 2010; Reddy et al., 1999), vibration (Alipour et al., 2010; Alipour and Shariyat, 2011a), and buckling (Shariyat and Alipour, 2013a; Alipour and Shariyat, 2013) analyses of plates under complicated conditions. Nevertheless, based on this type of theories, the transverse shear strains become constant in the thickness direction; so that the shear correction factors have to be used to correct the strain energy of the transverse shear stresses and consequently, adjust the transverse shear stiffness of the plate.

Various shear correction factors have been proposed so far to improve accuracy of the FSDT theories of the plates and beams. Timoshenko (1992) proposed a Poisson-ratio-dependent correction factor through matching the vibration frequencies obtained from the 2-D plane stress elasticity with those computed using the beam theory. Mindlin (1952) proposed constant and Poisson-ratio-dependent shear correction factors based on the free vibration data of the homogeneous and isotropic plates. An overview and elaborate discussion on the correction factors for flexural vibrations of the Timoshenko beams was presented by Kaneko (1975). Some shear correction factors had been derived for beams with various cross sections (Cowper, 1966; Murthy, 1970; Hutchinson, 1981; Rebello et al., 1983; Wittrick, 1987; Stephen, 1997; Pai and Schulz, 1999; Gruttmann and Wagner, 2001). Cowper (1966) used an approach based on the integration of the three-dimensional theory of elasticity, satisfying the boundary conditions of the cross-section. Based on the frequency matching approach, Hutchinson (1981) presented a shear correction factor through comparing results of Timoshenko beam theory and theory of elasticity. Rebello et al. (1983) analyzed vibration of bimodular sandwich beams with different behaviors in compression as compared to tension. Wittrick (1987) introduced different correction factors through comparing results of Mindlin's plate theory for the buckling under biaxial compression, free lateral vibration of a simply supported orthotropic rectangular plate, and static responses with those of the exact three-dimensional theory of elasticity. Ste-

phen (1997) found a correction factor through matching results of the flexural modes of the Mindlin finite plate theory with the Rayleigh-Lamb waves in the long wavelength limit. Pai and Schulz (1999) presented a shear correction factor for the isotropic beams by matching the exact shear stress resultants and shear strain energy with those of the first-order shear-deformation theory. Gruttman and Wangner (2001) derived a shear correction factors for arbitrary shaped cross section Timoshenko beams, based on equivalence of the strain energies calculated from the beam theory and the equilibrium equations. Hutchinson (2001) presented a new Timoshenko beam formulation and obtained a shear correction factor that depends on the Poisson ratio and the width to depth ratio. Efraim and Eisenberger (2007) proposed a new correction factor for the functionally graded plates through substituting the average Poisson ratio of the functionally graded mixture into the Poisson-ratio-dependent Mindlin's shear correction factor for the homogenous plate. Extending an approach previously used for the composite beams, Nguyen et al. (2008) proposed shear correction factors for the power-law FGM plates using the shear strain energy equivalence method. Chróścielewski, et al. (2010) suggested using two shear correction factors for the geometrically non-linear elastic regular and irregular shells. Menaa et al. (2012) used a concept similar to Nguyen et al. (2008), but presented an expression for plates made of sigmoid-law functionally graded materials.

Usage of the equivalent single-layer theories may lead to significant errors in analyzing the sandwich plates. In order to overcome restrictions of the equivalent single-layer theories, various layerwise and zigzag theories were presented. The zigzag theory (Shariyat and Alipour, 2013b; Alipour and Shariyat, 2011b, 2014a) with local linear through-thickness variations of the in-plane displacement components is a simple and computationally economic sandwich theory. However, using a constitutive-equations-based approach for this zigzag theory leads to constant layerwise transverse shear stresses. Therefore, using an appropriate shear-correction factor is a necessity to accurately determine the plate responses. The foregoing brief literature survey reveals that although various shear correction factors have been presented for the equivalent single-layer first-order shear-deformation beam/plate theories, no correction factor has been presented yet for the sandwich plates whose displacement fields vary locally. In the present paper, analytical local shear correction factors are proposed to modify the layerwise responses of each individual layer, especially when the layers are fabricated from functionally graded materials. In this regard, results of the employed zigzag theory, especially, the transverse shear stress are modified according to the three-dimensional theory of elasticity, instead of using the traditional constitutive-equations-based approach. The local shear correction factors are obtained using the strain energy equivalence method. Effects of the proposed shear correction factors are evaluated for free vibration analysis of the functionally graded sandwich circular plates, for various boundary conditions. The employed analytical method is Taylor transform method that is adequate for solution of the coupled differential equations (Alipour and Shariyat, 2010, 2011b, 2012, 2014a; Shariyat and Alipour, 2013b). Verification of the results has been accomplished through comparing present results with results of the three-dimensional theory of elasticity extracted from ABAQUS finite element code.

## 2 DESCRIPTION OF VARIATIONS OF THE MATERIAL PROPERTIES AND THE ZIGZAG DISPLACEMENT FIELD

Geometric parameters of the circular sandwich plate with functionally graded layers are shown in Fig.1. It is assumed that each layer of the sandwich plate is generally made of a mixture of ceramic and metallic constituent materials. Using a power–law for description of variations of the volume fraction of the metallic constituent material in the transverse direction, one may write:

$$V_m = \left(\frac{1}{2} - \frac{z}{h}\right)^g \tag{1}$$

So that:

$$V_c + V_m = 1 \tag{2}$$

where the subscripts $c$ and $m$ stand for ceramic and metal, respectively and $g$ is the positive definite volume fraction index. Therefore, $V_c$ and $V_m$ are the volume fractions of the ceramic and metallic constituent materials, respectively. According to Mori-Tanaka material properties model, variations of the bulk and shear moduli can be represented by:

$$\begin{cases} \dfrac{\mathrm{K}-\mathrm{K}_c}{\mathrm{K}_m-\mathrm{K}_c} = \dfrac{V_m}{1+(1-V_m)\dfrac{\mathrm{K}_m-\mathrm{K}_c}{\mathrm{K}_c+\frac{4}{3}G_c}}, \\ \dfrac{G-G_c}{G_m-G_c} = \dfrac{V_m}{1+(1-V_m)\dfrac{G_m-G_c}{G_c+f_c}}, \end{cases} \qquad f_c = \frac{G_c(9\mathrm{K}_c+8G_c)}{6(\mathrm{K}_c+2G_c)} \tag{3}$$

from which Young's modulus and Poisson's ratio may be determined as:

$$E = \frac{9\mathrm{K}G}{3\mathrm{K}+G}, \qquad \nu = \frac{3\mathrm{K}-2G}{6\mathrm{K}+2G} \tag{4}$$

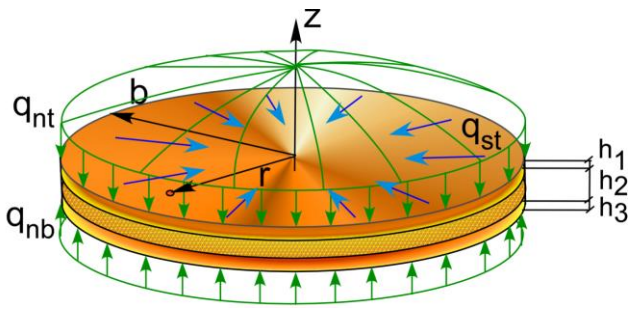


Figure 1: Geometric parameters of the considered circular sandwich plate with functionally graded layers.

Therefore, variations of the material properties within each layer may be determined from:

$$\begin{cases} \dfrac{K_1-K_{b1}}{K_{t1}-K_{b1}}=\dfrac{\left(\dfrac{z}{h_1}-\dfrac{h_2}{2h_1}\right)^{g_1}}{1+\dfrac{K_{t1}-K_{b1}}{K_{b1}+\frac{4}{3}G_{b1}}\left[1-\left(\dfrac{z}{h_1}-\dfrac{h_2}{2h_1}\right)^{g_1}\right]}, \\ \dfrac{G_1-G_{b1}}{G_{t1}-G_{b1}}=\dfrac{\left(\dfrac{z}{h_1}-\dfrac{h_2}{2h_1}\right)^{g_1}}{1+\dfrac{G_{t1}-G_{b1}}{G_{b1}+f_1}\left[1-\left(\dfrac{z}{h_1}-\dfrac{h_2}{2h_1}\right)^{g_1}\right]}, \ f_1=\dfrac{G_{b1}(9K_{b1}+8G_{b1})}{6K_{b1}+12G_{b1}} \end{cases} \quad \frac{h_2}{2}\le z\le \frac{h_2}{2}+h_1$$

$$\begin{cases} \dfrac{K_2-K_{b2}}{K_{t2}-K_{b2}}=\dfrac{\left(\dfrac{z}{h_2}+\dfrac{1}{2}\right)^{g_2}}{1+\dfrac{(K_{t2}-K_{b2})}{K_{b2}+\frac{4}{3}G_{b2}}\left[1-\left(\dfrac{z}{h_2}+\dfrac{1}{2}\right)^{g_2}\right]}, \\ \dfrac{G_2-G_{b2}}{G_{t2}-G_{b2}}=\dfrac{\left(\dfrac{z}{h_2}+\dfrac{1}{2}\right)^{g_2}}{1+\dfrac{G_{t2}-G_{b2}}{G_{b2}+f_2}\left[1-\left(\dfrac{z}{h_2}+\dfrac{1}{2}\right)^{g_2}\right]}, \ f_2=\dfrac{G_{b2}(9K_{b2}+8G_{b2})}{6K_{b2}+12G_{b2}} \end{cases} \quad -\frac{h_2}{2}\le z\le \frac{h_2}{2} \qquad (5)$$

$$\begin{cases} \dfrac{K_3-K_{t3}}{K_{b3}-K_{t3}}=\dfrac{\left(\dfrac{z}{h_3}+\dfrac{h_2}{2h_3}+1\right)^{g_3}}{1+\dfrac{K_{b3}-K_{t3}}{K_{t3}+\frac{4}{3}G_{t3}}\left[1-\left(\dfrac{z}{h_3}+\dfrac{h_2}{2h_3}+1\right)^{g_3}\right]}, \\ \dfrac{G_3-G_{t3}}{G_{b3}-G_{t3}}=\dfrac{\left(\dfrac{z}{h_3}+\dfrac{h_2}{2h_3}+1\right)^{g_3}}{1+\dfrac{G_{b3}-G_{t3}}{G_{t3}+f_3}\left[1-\left(\dfrac{z}{h_3}+\dfrac{h_2}{2h_3}+1\right)^{g_3}\right]}, \ f_3=\dfrac{G_{t3}(9K_{t3}+8G_{t3})}{6K_{t3}+12G_{t3}} \end{cases} \quad -\frac{h_2}{2}-h_3\le z\le -\frac{h_2}{2}$$

Although the traditional rule of mixtures is generally not appropriate for determination of the elastic moduli and Poisson's ratio, its application may be justified for modeling variations of the mass density within each layer (Shariyat and Jafari, 2013):

$$\rho = \rho_c V_c + \rho_m V_m \tag{6}$$

To enable accurately tracing the layerwise variations of the in-plane displacement component, a zigzag theory that is a result of a superposition of linear layerwise and linear global fields is adopted. So that variations of the resulting displacement field may be expressed as follows within each layer:

$$u^{(i)}(r,z,t) = u_g(r,z,t) + u_l^{(i)}(r,z,t), \qquad w = w_0 \tag{7}$$

where $u$ and $w$ are the radial and lateral displacement components. The subscripts $g$, $l$, and $0$ denote the global and local components and value of the displacement component at the reference plate, respectively. The $z$ coordinate is measured from the reference layer (e.g., the mid-plane of the plate) and positive upward. Imposing the interlaminar kinematic continuity conditions, the resulting displacement field of the sandwich plate may be expressed as follows:

$$\begin{aligned} u &= \begin{cases} u_0 + z\varphi_g + \left(z - \dfrac{h_2}{2}\right)\varphi_l^{(1)} + \dfrac{h_2}{2}\varphi_l^{(2)}, & \dfrac{h_2}{2} \le z \le \dfrac{h_2}{2} + h_1 \\ u_0 + z\varphi_g + z\varphi_l^{(2)}, & -\dfrac{h_2}{2} \le z \le \dfrac{h_2}{2} \\ u_0 + z\varphi_g + \left(z + \dfrac{h_2}{2}\right)\varphi_l^{(3)} - \dfrac{h_2}{2}\varphi_l^{(2)}, & -h_3 - \dfrac{h_2}{2} \le z \le -\dfrac{h_2}{2} \end{cases} \\ w &= w_0, \qquad -h_3 - \frac{h_2}{2} \le z \le \frac{h_2}{2} + h_1 \end{aligned} \tag{8}$$

where $\varphi_g$ and $\varphi_l^{(i)}, (i = 1,2,3)$ are the global rotation of the radial cross section and local rotations of the individual layers, respectively. $h_1$, $h_3$, and $h_2$ are thicknesses of the face sheets and core, respectively (Fig. 1). Eq. 8 may be rewritten as:

$$\begin{aligned} u &= \begin{cases} u_0 + \left(z - \dfrac{h_2}{2}\right)\psi^{(1)} + \dfrac{h_2}{2}\psi^{(2)}, & \dfrac{h_2}{2} \le z \le \dfrac{h_2}{2} + h_1 \\ u_0 + z\psi^{(2)}, & -\dfrac{h_2}{2} \le z \le \dfrac{h_2}{2} \\ u_0 + \left(z + \dfrac{h_2}{2}\right)\psi^{(3)} - \dfrac{h_2}{2}\psi^{(2)}, & -h_3 - \dfrac{h_2}{2} \le z \le -\dfrac{h_2}{2} \end{cases} \\ w &= w_0, \qquad -h_3 - \frac{h_2}{2} \le z \le \frac{h_2}{2} + h_1 \end{aligned} \tag{9}$$

where

$$\psi^{(i)} = \varphi_g + \varphi_l^{(i)} \tag{10}$$

## 3 DERIVATION OF THE LOCAL SHEAR CORRECTION FACTOR (LSCF)

In the present section, the local shear correction factors are derived for functionally graded circular sandwich plates with normal and shear tractions on the top and bottom surfaces. Although power-law variations are adopted for the volume fractions in the preceding section, present formulations may similarly be employed for any type of variations of the material properties.

For small deflections of axisymmetric circulate plates, the strain-displacement relations in the polar coordinate may be written as:

$$\varepsilon_r = \frac{\partial u}{\partial r},\ \varepsilon_\theta = \frac{u}{r},\ \gamma_{rz} = \frac{\partial u}{\partial z} + \frac{\partial w}{\partial r} \tag{11}$$

Since magnitude of the transverse normal strain is usually ignorable in comparison with that of the in-plane strains, the stress-strain relation of the $i$th layer may have the following form:

$$\begin{Bmatrix} \sigma_r^{(i)} \\ \sigma_\theta^{(i)} \\ \tau_{rz}^{(i)} \end{Bmatrix} = \begin{bmatrix} C_{11}^{(i)} & C_{12}^{(i)} & 0 \\ C_{21}^{(i)} & C_{22}^{(i)} & 0 \\ 0 & 0 & C_{33}^{(i)} \end{bmatrix} \begin{Bmatrix} \varepsilon_r^{(i)} \\ \varepsilon_\theta^{(i)} \\ \gamma_{rz}^{(i)} \end{Bmatrix} \qquad (i = 1,2,3) \tag{12}$$

where:

$$C_{11}^{(i)} = C_{22}^{(i)} = \frac{E^{(i)}\left(z^{(i)}\right)}{1-\left[\nu^{(i)}\left(z^{(i)}\right)\right]^2}, C_{12}^{(i)} = C_{21}^{(i)} = \frac{\nu^{(i)}\left(z^{(i)}\right)E_{(i)}\left(z^{(i)}\right)}{1-\left[\nu^{(i)}\left(z^{(i)}\right)\right]^2},\ C_{33}^{(i)} = \frac{E^{(i)}\left(z^{(i)}\right)}{2\left[1+\nu^{(i)}\left(z^{(i)}\right)\right]} \tag{13}$$

Based on the three-dimensional theory of elasticity, the equilibrium equations of the axisymmetric circular plate may be expressed as:

$$\frac{\partial \sigma_r}{\partial r} + \frac{\sigma_r - \sigma_\theta}{r} + \frac{\partial \tau_{rz}}{\partial z} = \rho \ddot{u} \tag{14}$$

$$\frac{1}{r}\frac{\partial (r\tau_{rz})}{\partial r} + \frac{\partial \sigma_z}{\partial z} = \rho \ddot{w} \tag{15}$$

where $\sigma_r$, $\sigma_\theta$ and $\sigma_z$ are the normal stresses and $\tau_{rz}$ is the transverse shear stress. Although the radial and transverse inertia body forces ( $\rho\ddot{u}$ and $\rho\ddot{w}$ ) appeared in Eqs. (14,15) may affect the shear correction factor, their effects may be ignored in comparison to those of the transversely applied distributed tractions, especially for the thin plates. This assumption has been employed in derivation of all of the available shear correction factors.

Based on Eq. 9, local variations of the in-plane displacement component of the $i$th layer may be rewritten as:

$$u^{(i)} = \hat{u}_0^{(i)} + \xi^{(i)}\hat{\varphi}_l^{(i)}; \qquad -\frac{h_i}{2} \le \xi^{(i)} \le \frac{h_i}{2} \tag{16}$$

where $\xi^{(i)}$ are the local z-coordinates of the layers that are measured from the mid-plane of the corresponding layer and are positive upward.

Based on Eqs. (11,12,16), the in-plane stress components will be:

$$\begin{cases} \sigma_r^{(i)} = C_{11}^{(i)}\left[\hat{u}_{0,r}^{(i)} + \xi^{(i)}\hat{\varphi}_{l,r}^{(i)} + \dfrac{v^{(i)}}{r}\left(\hat{u}_0^{(i)} + \xi^{(i)}\hat{\varphi}_l^{(i)}\right)\right] \\ \sigma_\theta^{(i)} = C_{11}^{(i)}\left[v^{(i)}\left(\hat{u}_{0,r}^{(i)} + \xi^{(i)}\hat{\varphi}_{l,r}^{(i)}\right) + \dfrac{1}{r}\left(\hat{u}_0^{(i)} + \xi^{(i)}\hat{\varphi}_l^{(i)}\right)\right] \end{cases} \tag{17}$$

By substituting Eq. (17) into Eq. (14), the radial equilibrium equation of each layer of the sandwich plate may be expressed based on the present zigzag theory as:

$$C_{11}^{(i)}\tilde{\nabla}^2\left(\hat{u}_0^{(i)} + \xi^{(i)}\hat{\varphi}_l^{(i)}\right) + \frac{\partial \tau_{rz}^{(i)}}{\partial \xi^{(i)}} = 0, \qquad \tilde{\nabla}^2 = \left(\frac{\partial^2}{\partial r^2} + \frac{1}{r}\frac{\partial}{\partial r} - \frac{1}{r^2}\right) \tag{18}$$

By integration of the elasticity equilibrium Eq. (18) across the plate thickness, the transverse shear stress within each layer may be obtained as:

$$\tau_{rz}^{(i)} = X^{(i)}\tilde{\nabla}^2\hat{u}_0^{(i)} + Y^{(i)}\tilde{\nabla}^2\hat{\varphi}_l^{(i)} + C^{(i)}, \qquad \begin{Bmatrix} X^{(i)} \\ Y^{(i)} \end{Bmatrix} = -\int C_{11}^{(i)} \begin{Bmatrix} 1 \\ \xi^{(i)} \end{Bmatrix} d\xi^{(i)} \tag{19}$$

$C^{(i)}$ is an integration constant. Integrating the transverse shear stress across the thickness of each layer, the transverse shear force per unit length of each layer can be obtained:

$$Q_r^{(i)} = \int_{-h_i/2}^{h_i/2} \tau_{rz}^{(i)} d\xi^{(i)} \tag{20}$$

For the general case where the top and bottom surfaces of the plate are subjected to simultaneous normal and shear tractions, the boundary and the continuity conditions of the in-plane displacement and transverse shear stress have to be satisfied:

$$\begin{cases} u^{(1)}_{\left(\xi=-\frac{h_1}{2}\right)} = u^{(2)}_{\left(\xi=\frac{h_2}{2}\right)} \\ u^{(3)}_{\left(\xi=\frac{h_3}{2}\right)} = u^{(2)}_{\left(\xi=-\frac{h_2}{2}\right)} \\ \tau^{(1)}_{rz\left(\xi=\frac{h_1}{2}\right)} = q_{st} \\ \tau^{(3)}_{rz\left(\xi=-\frac{h_3}{2}\right)} = q_{sb} \\ \tau^{(1)}_{rz\left(\xi=-\frac{h_1}{2}\right)} = \tau^{(2)}_{rz\left(\xi=\frac{h_2}{2}\right)} \\ \tau^{(3)}_{rz\left(\xi=\frac{h_3}{2}\right)} = \tau^{(2)}_{rz\left(\xi=-\frac{h_2}{2}\right)} \end{cases} \tag{21}$$

where $q_{st}$ and $q_{sb}$ are the shear tractions of the top and bottom surfaces of the sandwich plate. Therefore:

$$C^{(1)} = q_{st},\ C^{(2)} = \tau^{(1)}_{rz\left(\xi=\frac{h_2}{2}\right)},\ C^{(1)} = q_{sb}, \tag{22}$$

Using the Eqs. (20,21), the unknown displacement parameters $\widehat{u}_0^{(i)}$ and , $\widehat{\varphi}_l^{(i)}$ may be obtained based on the shear force of the relevant layer per unit length. On the other hand, based on Eq. (15) and the boundary and continuity conditions (at the interfaces between layers):

$$\begin{aligned} \sigma_z^{(1)} &= \frac{1}{r}\int_z^{h_3/2} \frac{\partial(r\tau_{rz}^{(1)})}{\partial r} d\xi + q_{nt} \\ \sigma_z^{(2)} &= \frac{1}{r}\int_z^{h_2/2} \frac{\partial(r\tau_{rz}^{(2)})}{\partial r} d\xi + \sigma_{z\left(\xi=\frac{h_2}{2}\right)}^{(1)} \\ \sigma_z^{(3)} &= \frac{1}{r}\int_z^{-h_2/2} \frac{\partial(r\tau_{rz}^{(3)})}{\partial r} d\xi + q_{nb} \end{aligned} \tag{23}$$

$q_{nt}$ and $q_{nb}$ are the normal tractions of the top and bottom surfaces of the sandwich plate (Fig. 1). The transverse distributions of the transverse shear and normal stresses may be determined based on computing the integrals appeared in Eqs. (20) and (23) for each loading case. However, for the special case of a sandwich plate whose material properties are constant within each layer, the through-thickness variations of the transverse shear stress can be determined explicitly as:

$$\tau_{rz}^{(1)}=\frac{3}{4}\frac{1}{h_1^3h_2h_3\left[3h_1h_3\eta_1\eta_3+4h_2\eta_2\left(h_1\eta_1+h_2\eta_2+h_3\eta_3\right)\right]}\Big\{h_1^3h_2\eta_1\eta_2\left(h_1h_2Q_3+8h_2h_3Q_1-2h_1h_3Q_2\right)$$
$$+h_1^3h_3^2\eta_1\eta_3\left(6h_2Q_1-h_1Q_2\right)+6h_1^2h_2^2h_3Q_1\left(h_2\eta_2^2+h_3\eta_2\eta_3\right)+\Big[4h_1^3\eta_1\left(h_2^2\eta_2Q_3-h_3^2\eta_3Q_2-2h_2h_3\eta_2Q_2\right)$$
$$-8h_1h_2^2h_3\eta_2Q_1\left(h_3\eta_3+h_2\eta_2\right)\Big]\xi^{(1)}+\Big[8h_3h_2\eta_2\left(3h_1^2\eta_1Q_2-h_2^2\eta_2Q_1-4h_1h_2\eta_1Q_1-h_2h_3\eta_3Q_1\right)$$
$$+4h_1h_3^2\eta_1\eta_3\left(3h_1Q_2-6h_2Q_1\right)-12h_1^2h_2^2\eta_1\eta_2Q_3\Big]\xi^{(1)2}\Big\}+q_{st}$$

$$\tau_{rz}^{(2)}=\frac{3}{4}\frac{1}{h_1h_2^2h_3\left[3h_1h_3\eta_1\eta_3+4h_2\eta_2\left(h_1\eta_1+h_2\eta_2+h_3\eta_3\right)\right]}\Big\{6h_2^2\eta_2Q_2\left(h_1^2h_3\eta_1+h_1h_3^2\eta_3\right)$$
$$-h_2^3\eta_2\left(h_1^2\eta_1Q_3+h_3^2\eta_3Q_1\right)-2h_2^4\eta_2^2\left(h_1Q_3+h_3Q_1\right)+8h_1h_2^3h_3\eta_2^2Q_2+4h_1^2h_2h_3^2h_3\eta_1\eta_3Q_2$$
$$+\Big[12h_2^2\eta_2\left(h_3^2\eta_3Q_1-h_1^2\eta_1Q_3\right)+8h_2\eta_2Q_2\left(h_1^2h_3\eta_1-h_1h_3^2\eta_3\right)-8\eta_2^2h_2^3\left(h_1Q_3-h_3Q_1\right)\Big]\xi^{(2)} \qquad (24)$$
$$+\Big[12h_2\eta_2\left(h_1^2\eta_1Q_3+h_3^2\eta_3Q_1\right)-8\eta_2Q_2\left(h_1^2h_3\eta_1+h_1h_3^2\eta_3\right)+24\eta_2^2h_2^2\left(h_1Q_3+h_3Q_1\right)-32h_1h_2h_3\eta_2^2Q_2\Big]\xi^{(2)2}\Big\}$$
$$+\tau_{rz}^{(1)}{}_{\left(\xi=\frac{h_2}{2}\right)}$$

$$\tau_{rz}^{(3)}=\frac{3}{4}\frac{1}{h_1h_2h_3^3\left[3h_1h_3\eta_1\eta_3+4h_2\eta_2\left(h_1\eta_1+h_2\eta_2+h_3\eta_3\right)\right]}\Big\{h_2h_3^3\eta_2\eta_3\left(h_2h_3Q_1+8h_1h_2Q_3-2h_1h_3Q_2\right)$$
$$+h_1^2h_3^3\eta_1\eta_3\left(6h_2Q_3-h_3Q_2\right)+6h_1h_2^2h_3^2Q_3\left(h_2\eta_2^2+h_1\eta_1\eta_2\right)+\Big[4h_3^3\eta_3\left(h_1^2\eta_1Q_2+2h_1h_2\eta_2Q_2-h_2^2\eta_2Q_1\right)$$
$$+8h_1h_2^2h_3\eta_2Q_3\left(h_1\eta_1+h_2\eta_2\right)\Big]\xi^{(3)}+\Big[8h_1h_2\eta_2\left(3h_3^2\eta_3Q_2-h_2^2\eta_2Q_3-4h_2h_3\eta_3Q_3-h_1h_2\eta_1Q_3\right)$$
$$+4h_1^2h_3\eta_1\eta_3\left(3h_3Q_2-6h_2Q_3\right)-12h_2^2h_3^2\eta_2\eta_3Q_1\Big]\xi^{(3)2}\Big\}+q_{sb}$$

where $\eta_i=\dfrac{E^{(i)}{}_i}{1-\nu^{(i)2}}$.

On the other hand, based on the present first-order zigzag theory, the constitutive-equations-based transverse shear stress of each layer is:

$$\tau_{rz}'^{(i)}=G^{(i)}(\xi^{(i)})\left(\bar{\varphi}_l^{(i)}+w_{,r}\right) \qquad (25)$$

By integration of Eq. (25) across the plate thickness, the transverse shear force of each layer per unit length may be obtained as:

$$Q_r^{(i)} = \int_{-h_i/2}^{h_i/2} \tau_{rz}^{\prime(i)} d\xi^{(i)} = \kappa^{(i)} L^{(i)} \left( \widehat{\varphi}_l^{(i)} + w_{,r} \right), \qquad \mathcal{G}^{(i)} = \int_{-h_i/2}^{h_i/2} G^{(i)}(\xi^{(i)}) d\xi^{(i)} \tag{26}$$

where $\kappa^{(i)}$ is the local shear correction factor of the $i$th layer. Based on Eq. (26), Eq. (25) may be rewritten in terms of the shear force per length as:

$$\tau_{rz}^{\prime(i)} = \frac{G^{(i)}\left(\xi^{(i)}\right)}{\mathcal{G}^{(i)}} Q_r^{(i)} \tag{27}$$

The strain energy associated with the elasticity-based transverse shear stress (19) can be determined from the following equation:

$$U_s^{(i)} = \frac{1}{2} \int_0^b \int_{-h_i/2}^{h_i/2} \frac{1}{G^{(i)}\left(\xi^{(i)}\right)} \tau_{rz}^{(i)2} 2\pi r \, dr d\xi^{(i)} \tag{28}$$

On the other hand, the strain energy associated with the constitutive-equations-based transverse shear stress maybe corrected as follows to match Eq. (28):

$$\tilde{U}_s^{(i)} = \frac{1}{2} \int_0^b \int_{-h_i/2}^{h_i/2} \frac{G^{(i)}\left(\xi^{(i)}\right)}{\kappa^{(i)} \mathcal{G}^{(i)2}} Q_r^{(i)2} 2\pi r dr d\xi^{(i)} \tag{29}$$

Equating the strain energy expressions appeared in Eqs. (28,29) leads to the following set of new general local correction factors for the three-layer functionally graded sandwich plate.

$$\kappa^{(i)} = \frac{\int_0^b \int_{-h_i/2}^{h_i/2} \frac{G^{(i)}\left(\xi^{(i)}\right)}{\mathcal{G}^{(i)2}} Q_r^{(i)2} 2\pi r \, dr d\xi^{(i)}}{\int_0^b \int_{-h_i/2}^{h_i/2} \frac{1}{G^{(i)}\left(\xi^{(i)}\right)} \tau_{rz}^{(i)2} 2\pi r \, dr d\xi^{(i)}} \tag{30}$$

In the obtained correction factors, effects of gradation of the material properties, geometric parameters, and the tractions of the sandwich plate are considered. Moreover, since the correction factors are presented in terms of the shear loads per unit length, an elasticity-based correction is required for determination of the accurate transverse shear stress, as explained in the next section. In the special cases where the top and bottom surfaces of the plate are free of shear tractions and each layer is fabricated from a homogeneous isotropic material, the following explicit expressions may be used for the shear correction factors:

$$\kappa^{(1)}=\int_0^b\Big\{\frac{5}{3}Q_1^2h_2^3h_3^3\big[4\chi_2(\chi_1+\chi_3+\chi_2)+3\chi_1\chi_3\big]^2\Big/\Big\{\big[4\chi_1\chi_2-4\chi_2^2-4\chi_2\chi_3-3\chi_1\chi_3\big]\chi_1\chi_2h_1h_2^2h_3Q_1Q_3$$
$$+\Big[\chi_2^2\Big(32\Big(\chi_1^2+\chi_2^2+\chi_3^2\Big)+56\chi_1\chi_2+64\chi_2\chi_3+98\chi_1\chi_3\Big)+6\chi_1\chi_3\big(8\chi_1\chi_2+3\chi_1\chi_3+7\chi_2\chi_3\big)\Big]h_2^2h_3^2Q_1^2$$
$$-\Big[\chi_1\Big(3\chi_3^2+8\chi_2^2+10\chi_2\chi_3\Big)-8\chi_2^3-4\chi_2\chi_3^2-12\chi_3\chi_2^2\Big]h_1h_2h_3^2\chi_1Q_1Q_2-\Big(2\chi_2^2+\chi_2\chi_3\Big)4h_1^2h_2h_3\chi_1^2Q_2Q_3$$
$$+\Big(\chi_2\chi_3+\chi_2^2\Big)8h_1^2h_3^2\chi_1^2Q_2^2+2\chi_1^2\chi_2^2h_1^2h_2^2Q_3^2\Big\}\Big\}dr$$

$$\kappa^{(2)}=\int_{0_i}^b\Big\{\frac{5}{3}Q_2^2h_1^3h_3^3\big[4\chi_2(\chi_1+\chi_3+\chi_2)+3\chi_1\chi_3\big]^2\Big/\Big\{-\big[4\chi_2^2+12\chi_2\chi_3+12\chi_1\chi_2+21\chi_1\chi_3\big]h_1h_2^3h_3\chi_2^2Q_1Q_3$$
$$+\Big[\Big(4\chi_1\chi_2-4\chi_2^2-8\chi_3^2-8\chi_2\chi_3+7\chi_1\chi_3\Big)h_3Q_1+\Big(4\chi_2\chi_3-4\chi_2^2-8\chi_1^2-8\chi_1\chi_2+7\chi_1\chi_3\Big)h_1Q_3\Big]2h_1h_2h_3\chi_2^2Q_2$$
$$+\Big[40\chi_2\Big(\chi_1\chi_3^2+\chi_1^2\chi_3\Big)+32\chi_2^2\Big(\chi_1^2+\chi_2^2+\chi_3^2\Big)+56\chi_2^3(\chi_1+\chi_3)+84\chi_1\chi_2^2\chi_3+15\chi_1^2\chi_3^2\Big]h_1^2h_3^2Q_2^2$$
$$+\Big[6\chi_3^2+9\chi_2\chi_3+4\chi_2^2\Big]2h_2^2h_3^2\chi_2^2Q_1^2+\Big[6\chi_1^2+9\chi_1\chi_2+4\chi_2^2\Big]2h_1^2h_2^2\chi_2^2Q_3^2\Big\}\Big\}dr \qquad (31)$$

$$\kappa^{(3)}=\int_0^b\Big\{\frac{5}{3}Q_3^2h_1^3h_2^3\big[4\chi_2(\chi_1+\chi_3+\chi_2)+3\chi_1\chi_3\big]^2\Big/\Big\{\big[4\chi_3\chi_2-4\chi_2^2-4\chi_2\chi_1-3\chi_1\chi_3\big]\chi_3\chi_2h_3h_2^2h_3Q_1Q_3$$
$$+\Big[\chi_2^2\Big(32\Big(\chi_1^2+\chi_2^2+\chi_3^2\Big)+56\chi_2\chi_3+64\chi_1\chi_2+98\chi_1\chi_3\Big)+6\chi_1\chi_3\big(8\chi_2\chi_3+3\chi_1\chi_3+7\chi_1\chi_2\big)\Big]h_1^2h_2^2Q_3^2$$
$$-\Big[\chi_3\Big(3\chi_1^2+8\chi_2^2+10\chi_1\chi_2\Big)-8\chi_2^3-4\chi_1^2\chi_2-12\chi_1\chi_2^2\Big]h_1^2h_2h_3\chi_3Q_2Q_3-\Big(2\chi_2^2+\chi_1\chi_2\Big)4h_1h_2h_3^2\chi_3^2Q_1Q_2$$
$$+\Big(\chi_1\chi_2+\chi_2^2\Big)8h_1^2h_3^2\chi_3^2Q_2^2+2\chi_2^2\chi_3^2h_2^2h_3^2Q_1^2\Big\}\Big\}dr$$

where $\chi_i=\dfrac{h_iE^{(i)}{}_i}{1-\nu^{(i)2}}$.

Therefore, after finding the transverse shear stresses, through-thickness variations of the transverse normal stress can be determined from:

$$\sigma_z^{(1)}=\frac{3}{4}\frac{1}{h_1^3h_2h_3\left[3h_1h_3\eta_1\eta_3+4h_2\eta_2\left(h_1\eta_1+h_2\eta_2+h_3\eta_3\right)\right]}\Bigg\{h_1^3h_2\eta_1\eta_2\left(8h_2h_3\tilde{Q}_1-2h_1h_3\tilde{Q}_2+h_1h_2\tilde{Q}_3\right)$$
$$+h_1^3h_3^2\eta_1\eta_3\left(6h_2\tilde{Q}_1-h_1\tilde{Q}_2\right)+6h_1^2h_2^2h_3\tilde{Q}_1\left(h_2\eta_2^2+h_3\eta_2\eta_3\right)+\Big[4h_1^3\eta_1\left(h_2^2\eta_2\tilde{Q}_3-h_3^2\eta_3\tilde{Q}_2-2h_2h_3\eta_2\tilde{Q}_2\right)$$
$$-8h_1h_2^2h_3\eta_2\tilde{Q}_1\left(h_3\eta_3+h_2\eta_2\right)\Big]\left(\frac{h_1^2}{8}-\frac{\xi^{(1)2}}{2}\right)+\Big[8h_3h_2\eta_2\left(3h_1^2\eta_1\tilde{Q}_2-h_2^2\eta_2\tilde{Q}_1-4h_1h_2\eta_1\tilde{Q}_1-h_2h_3\eta_3\tilde{Q}_1\right)$$
$$+4h_1h_3^2\eta_1\eta_3\left(3h_1\tilde{Q}_2-6h_2\tilde{Q}_1\right)-12h_1^2h_2^2\eta_1\eta_2\tilde{Q}_3\Big]\left(\frac{h_1^3}{24}-\frac{\xi^{(1)3}}{3}\right)\Bigg\}+q_{nt}$$

$$\sigma_z^{(2)}=\frac{3}{4}\frac{1}{h_1h_2^2h_3\left[3h_1h_3\eta_1\eta_3+4h_2\eta_2\left(h_1\eta_1+h_2\eta_2+h_3\eta_3\right)\right]}\Bigg\{6h_2^2\eta_2\tilde{Q}_2\left(h_1^2h_3\eta_1+h_1h_3^2\eta_3\right)$$
$$-h_2^3\eta_2\left(h_1^2\eta_1\tilde{Q}_3+h_3^2\eta_3\tilde{Q}_1\right)-2h_2^4\eta_2^2\left(h_1\tilde{Q}_3+h_3\tilde{Q}_1\right)+8h_1h_2^3h_3\eta_2^2\tilde{Q}_2+4h_1^2h_2h_3^2h_3\eta_1\eta_3\tilde{Q}_2$$
$$+\Big[12h_2^2\eta_2\left(h_3^2\eta_3\tilde{Q}_1-h_1^2\eta_1\tilde{Q}_3\right)+8h_2\eta_2\tilde{Q}_2\left(h_1^2h_3\eta_1-h_1h_3^2\eta_3\right)-8\eta_2^2h_2^3\left(h_1\tilde{Q}_3-h_3\tilde{Q}_1\right)\Big]\left(\frac{h_2^2}{8}-\frac{\xi^{(2)2}}{2}\right) \tag{32}$$
$$+\Big[12h_2\eta_2\left(h_1^2\eta_1\tilde{Q}_3+h_3^2\eta_3\tilde{Q}_1\right)-8\eta_2\tilde{Q}_2\left(h_1^2h_3\eta_1+h_1h_3^2\eta_3\right)+24\eta_2^2h_2^2\left(h_1\tilde{Q}_3+h_3\tilde{Q}_1\right)$$
$$-32h_1h_2h_3\eta_2^2\tilde{Q}_2\left(\frac{h_2^3}{24}-\frac{\xi^{(2)3}}{3}\right)\Bigg\}+\sigma_z^{(1)}{}_{\left(\xi^{(1)}=\frac{h_1}{2}\right)}$$

$$\sigma_z^{(3)}=\frac{3}{4}\frac{1}{h_1h_2h_3^3\left[3h_1h_3\eta_1\eta_3+4h_2\eta_2\left(h_1\eta_1+h_2\eta_2+h_3\eta_3\right)\right]}\Bigg\{h_2h_3^3\eta_2\eta_3\left(h_2h_3\tilde{Q}_1+8h_1h_2\tilde{Q}_3-2h_1h_3\tilde{Q}_2\right)$$
$$+h_1^2h_3^3\eta_1\eta_3\left(6h_2\tilde{Q}_3-h_3\tilde{Q}_2\right)+6h_1h_2^2h_3^2\tilde{Q}_3\left(h_2\eta_2^2+h_1\eta_1\eta_2\right)+\Big[4h_3^3\eta_3\left(h_1^2\eta_1\tilde{Q}_2+2h_1h_2\eta_2\tilde{Q}_2-h_2^2\eta_2\tilde{Q}_1\right)$$
$$+8h_1h_2^2h_3\eta_2\tilde{Q}_3\left(h_1\eta_1+h_2\eta_2\right)\Big]\left(\frac{h_3^2}{8}-\frac{\xi^{(3)2}}{2}\right)+\Big[4h_1^2h_3\eta_1\eta_3\left(3h_3\tilde{Q}_2-6h_2\tilde{Q}_3\right)-12h_2^2h_3^2\eta_2\eta_3\tilde{Q}_1$$
$$+8h_1h_2\eta_2\left(3h_3^2\eta_3\tilde{Q}_2-h_2^2\eta_2\tilde{Q}_3-4h_2h_3\eta_3\tilde{Q}_3-h_1h_2\eta_1\tilde{Q}_3\right)\Big]\left(-\frac{h_3^3}{24}-\frac{\xi^{(3)3}}{3}\right)\Bigg\}+q_{nb}$$

and:

$$\tilde{Q}_i=Q_{i,r}+\frac{Q_i}{r} \tag{33}$$

Even though investigation of the transverse normal stresses is not the main aim of the present paper, since their expressions are indirect outcomes of the present research and have not derived by other researchers, they are included to increase the fruitfulness of the paper.

## 4 GOVERNING EQUATIONS OF FREE VIBRATION OF THE FUNCTIONALLY GRADED CIRCULAR SANDWICH PLATE

The governing equations of the free vibration of the sandwich plate may be derived by either using the minimum total potential energy principle or Hamilton's principle. Based on the first approach, one may write:

$$\delta\Pi = \delta U + \delta K = 0 \tag{34}$$

where $\delta\Pi$, $\delta U$, and $\delta K$ are increments of the total potential energy, strain energy, and kinetic energy (energy of the inertial loads), respectively:

$$\begin{gathered}\delta U = \int_V \delta\varepsilon^T \sigma\, dV = \frac{1}{2}\int_V (\sigma_r \delta\varepsilon_r + \sigma_\theta \delta\varepsilon_\theta + \tau_{rz}\delta\gamma_{rz})dV, \\ \delta K = \int_V \rho\left(\ddot{u}\delta u + \ddot{w}\delta w\right)dV\end{gathered} \tag{35}$$

Employing the minimum total potential energy principle taking into account Eqs. (9,11,12), leads to the following five coupled governing equations of motion of the circular sandwich plate in the cylindrical coordinate system ($r$, $\vartheta$, $z$):

$$\begin{gathered}\delta u_0 \neq 0: \\ (A^{(1)} + A^{(2)} + A^{(3)})\tilde{\nabla}^2 u_0 + \left(B^{(1)} - \frac{h_2}{2}A^{(1)}\right)\tilde{\nabla}^2\psi^{(1)} + \left(\frac{h_2}{2}A^{(1)} + B^{(2)} - \frac{h_2}{2}A^{(3)}\right)\tilde{\nabla}^2\psi^{(2)} \\ + \left(B^{(3)} + \frac{h_2}{2}A^{(3)}\right)\tilde{\nabla}^2\psi^{(3)} = \left(I_0^{(1)} + I_0^{(2)} + I_0^{(3)}\right)\ddot{u}_0 + \left(I_1^{(1)} - \frac{h_2}{2}I_0^{(1)}\right)\ddot{\psi}^{(1)} \\ + \left[\frac{h_2}{2}\left(I_0^{(1)} - I_0^{(3)}\right) + I_1^{(2)}\right]\ddot{\psi}^{(2)} + \left(I_1^{(3)} + \frac{h_2}{2}I_0^{(3)}\right)\ddot{\psi}^{(3)}\end{gathered} \tag{36-a}$$

$$\begin{gathered}\delta\psi^{(1)} \neq 0: \\ \left(B^{(1)} - \frac{h_2}{2}A^{(1)}\right)\tilde{\nabla}^2 u_0 + \left[\left(\frac{h_2}{2}\right)^2 A^{(1)} - h_2 B^{(1)} + D^{(1)}\right]\tilde{\nabla}^2\psi^{(1)} + \frac{h_2}{2}\left(B^{(1)} - \frac{h_2}{2}A^{(1)}\right)\tilde{\nabla}^2\psi^{(2)} - \kappa^{(1)}\bar{A}^{(1)} \\ \left(\psi^{(1)} + \frac{\partial w}{\partial r}\right) = \left(I_1^{(1)} - \frac{h_2}{2}I_0^{(1)}\right)\ddot{u}_0 + \frac{h_2}{2}\left(I_1^{(1)} - \frac{h_2}{2}I_0^{(1)}\right)\ddot{\psi}^{(2)} + \left[I_2^{(1)} - h_2 I_1^{(1)} + \left(\frac{h_2}{2}\right)^2 I_0^{(1)}\right]\ddot{\psi}^{(1)}\end{gathered} \tag{36-b}$$

$\delta\psi^{(2)} \neq 0$ :

$$\left(\frac{h_2}{2}(A^{(1)}-A^{(3)})+B^{(2)}\right)\tilde{\nabla}^2 u_0+\frac{h_2}{2}\left(B^{(1)}-\frac{h_2}{2}A^{(1)}\right)\tilde{\nabla}^2\psi^{(1)}+\left[\left(\frac{h_2}{2}\right)^2(A^{(1)}+A^{(3)})+D^{(2)}\right]$$
$$\tilde{\nabla}^2\psi^{(2)}-\frac{h_2}{2}\left(B^{(3)}+\frac{h_2}{2}A^{(3)}\right)\tilde{\nabla}^2\psi^{(3)}-\kappa^{(2)}\bar{A}^{(2)}\left(\psi^{(2)}+\frac{\partial w}{\partial r}\right)=\left(\frac{h_2}{2}I_0^{(1)}+I_1^{(2)}-\frac{h_2}{2}I_0^{(3)}\right)\ddot{u}_0 \qquad (36\text{-c})$$
$$+\frac{h_2}{2}\left(I_1^{(1)}-\frac{h_2}{2}I_0^{(1)}\right)\ddot{\psi}^{(1)}+\left[\left(\frac{h_2}{2}\right)^2(I_0^{(1)}+I_0^{(3)})+I_2^{(2)}\right]\ddot{\psi}^{(2)}-\frac{h_2}{2}\left(I_1^{(3)}+\frac{h_2}{2}I_0^{(3)}\right)\ddot{\psi}^{(3)}$$

$\delta\psi^{(3)} \neq 0$ :

$$\left(B^{(3)}+\frac{h_2}{2}A^{(3)}\right)\tilde{\nabla}^2 u_0-\frac{h_2}{2}\left(\frac{h_2}{2}A^{(3)}+B^{(3)}\right)\tilde{\nabla}^2\psi^{(2)}+\left(D^{(3)}+\frac{h_2}{2}2B^{(3)}+\frac{h_2}{2}A^{(3)}\right)\tilde{\nabla}^2\psi^{(3)}$$
$$-\kappa^{(3)}\bar{A}^{(3)}\left(\psi^{(3)}+\frac{\partial w}{\partial r}\right)=\left(I_1^{(3)}-\frac{h_3}{2}I_0^{(3)}\right)\ddot{u}_0+\left[I_2^{(3)}+h_2 I_1^{(3)}+\left(\frac{h_2}{2}\right)^2 I_0^{(3)}\right]\ddot{\psi}^{(3)} \qquad (36\text{-d})$$
$$-\frac{h_2}{2}\left(\frac{h_2}{2}I_0^{(3)}+I_1^{(3)}\right)\ddot{\psi}^{(2)}$$

$\delta w \neq 0$ :

$$\left(\kappa^{(1)}\bar{A}^{(1)}+\kappa^{(2)}\bar{A}^{(2)}+\kappa^{(3)}\bar{A}^{(3)}\right)\left(\frac{\partial^2 w}{\partial r^2}+\frac{1}{r}\frac{\partial w}{\partial r}\right)+\kappa^{(1)}\bar{A}^{(1)}\left(\frac{\partial\psi^{(1)}}{\partial r}+\frac{\psi^{(1)}}{r}\right)$$
$$+\kappa^{(2)}\bar{A}^{(2)}\left(\frac{\partial\psi^{(2)}}{\partial r}+\frac{\psi^{(2)}}{r}\right)+\kappa^{(3)}\bar{A}^{(3)}\left(\frac{\partial\psi^{(3)}}{\partial r}+\frac{\psi^{(3)}}{r}\right)=(I_0^{(1)}+I_0^{(2)}+I_0^{(3)})\ddot{w} \qquad (36\text{-e})$$

The resulting essential and natural boundary conditions are:

▷ $\delta u_0 = 0$

or

▷ $\left(A^{(1)}+A^{(2)}+A^{(3)}\right)\frac{\partial u_0}{\partial r}+\frac{1}{r}\left(\tilde{A}^{(1)}+\tilde{A}^{(2)}+\tilde{A}^{(3)}\right)u_0+\left(\frac{h_1}{2}A^{(1)}+B^{(1)}\right)\frac{\partial \psi^{(1)}}{\partial r}+\frac{1}{r}\left(\tilde{B}^{(1)}-\frac{h_2}{2}\tilde{A}^{(1)}\right)$
$\psi^{(1)}+\left(\frac{h_2}{2}A^{(1)}+B^{(2)}-\frac{h_2}{2}A^{(3)}\right)\frac{\partial \psi^{(2)}}{\partial r}+\frac{1}{r}\left(\tilde{B}^{(3)}+\frac{h_2}{2}\tilde{A}^{(3)}\right)\psi^{(3)}+\left(B^{(3)}+\frac{h_2}{2}A^{(3)}\right)\frac{\partial \psi^{(3)}}{\partial r}$
$+\frac{1}{r}\left(\frac{h_2}{2}\tilde{A}^{(1)}+\tilde{B}^{(2)}-\frac{h_2}{2}\tilde{A}^{(3)}\right)\psi^{(2)}=0$ (37-a)

▷ $\delta \psi^{(1)} = 0$

or

▷ $\left(-\frac{h_2}{2}A^{(1)}+B^{(1)}\right)\frac{\partial}{\partial r}\left(u_0-\frac{h_2}{2}\psi^{(1)}+\frac{h_2}{2}\psi^{(2)}\right)+\left(D^{(1)}-\frac{h_2}{2}B^{(1)}\right)\frac{\partial \psi^{(1)}}{\partial r}+\frac{1}{r}\left(\tilde{B}^{(1)}-\frac{h_2}{2}\tilde{A}^{(1)}\right)$
$\left(u_0-\frac{h_2}{2}\psi^{(1)}+\frac{h_2}{2}\psi^{(2)}\right)+\frac{1}{r}\left(\tilde{D}^{(1)}-\frac{h_2}{2}\tilde{B}^{(1)}\right)\psi^{(1)}=0$ (37-b)

▷ $\delta \psi^{(2)} = 0$

or

▷ $\frac{h_2}{2}A^{(1)}\frac{\partial}{\partial r}\left(u_0-\frac{h_2}{2}\psi^{(1)}+\frac{h_2}{2}\psi^{(2)}\right)+\frac{h_2}{2r}\tilde{A}^{(1)}\left(u_0-\frac{h_2}{2}\psi^{(1)}+\frac{h_2}{2}\psi^{(2)}\right)+\frac{h_2}{2}B^{(1)}\frac{\partial \psi^{(1)}}{\partial r}$
$+\frac{1}{r}\frac{h_2}{2}\tilde{B}^{(1)}\psi^{(1)}+B^{(2)}\frac{\partial u_0}{\partial r}+\frac{1}{r}\tilde{B}^{(2)}u_0+D^{(2)}\frac{\partial \psi^{(2)}}{\partial r}-\frac{h_2}{2}A^{(3)}\frac{\partial}{\partial r}\left(u_0+\frac{h_2}{2}\psi^{(3)}-\frac{h_2}{2}\psi^{(2)}\right)$
$+\frac{1}{r}\tilde{D}^{(2)}\psi^{(2)}-\frac{h_2}{2}\frac{1}{r}\tilde{A}^{(3)}\left(u_0+\frac{h_2}{2}\psi^{(3)}-\frac{h_2}{2}\psi^{(2)}\right)-\frac{h_2}{2}B^{(3)}\frac{\partial \psi^{(3)}}{\partial r}-\frac{h_2}{2}\frac{1}{r}\tilde{B}^{(3)}\psi^{(3)}=0$ (37-c)

▷ $\delta \psi^{(3)} = 0$

or

▷ $\left(B^{(3)}+\frac{h_2}{2}A^{(3)}\right)\left(u_{0,r}+\frac{h_2}{2}\psi^{(3)}_{,r}-\frac{h_2}{2}\psi^{(2)}_{,r}\right)+\left(D^{(3)}+\frac{h_2}{2}B^{(3)}\right)\psi^{(3)}_{,r}+\frac{1}{r}\left(\tilde{B}^{(3)}+\frac{h_2}{2}\tilde{A}^{(3)}\right)$
$\left(u_0+\frac{h_2}{2}\psi^{(3)}-\frac{h_2}{2}\psi^{(2)}\right)+\frac{1}{r}\left(\tilde{D}^{(3)}+\frac{h_2}{2}\tilde{B}^{(3)}\right)\psi^{(3)}=0$ (37-d)

▷ $w = 0$

or

▷ $\left(\kappa^{(1)}\overline{A}^{(1)}+\kappa^{(2)}\overline{A}^{(2)}+\kappa^{(3)}\overline{A}^{(3)}\right)w_{,r}+\kappa^{(1)}\overline{A}^{(1)}\psi^{(1)}+\kappa^{(2)}\overline{A}^{(2)}\psi^{(2)}+\kappa^{(3)}\overline{A}^{(3)}\psi^{(3)}=0$ (37-e)

where

$$\begin{Bmatrix} A^{(i)} \\ B^{(i)} \\ D^{(i)} \end{Bmatrix} = \int_{-\frac{h_i}{2}}^{\frac{h_i}{2}} \frac{E^{(i)}}{1-\nu^{(i)2}} \begin{Bmatrix} 1 \\ \xi^{(i)} \\ \xi^{(i)2} \end{Bmatrix} d\xi^{(i)}, \begin{Bmatrix} \tilde{A}^{(i)} \\ \tilde{B}^{(i)} \\ \tilde{D}^{(i)} \end{Bmatrix} = \int_{-\frac{h_i}{2}}^{\frac{h_i}{2}} \frac{\nu^{(i)}E^{(i)}}{1-\nu^{(i)2}} \begin{Bmatrix} 1 \\ \xi^{(i)} \\ \xi^{(i)2} \end{Bmatrix} d\xi^{(i)}, \ \bar{A}^{(i)} = \int_{-\frac{h_i}{2}}^{\frac{h_i}{2}} \frac{E^{(i)}}{2(1+\nu^{(i)})} d\xi^{(i)} \qquad i=1,2,3$$

$$I_j^{(i)} = \int_{-\frac{h_i}{2}}^{\frac{h_i}{2}} \rho^{(i)} \xi^{(i)j} d\xi^{(i)}; \qquad i=1,2,3;\ j=0,1,2 \tag{38}$$

## 5 DEVELOPMENT OF TAYLOR'S TRANSFORM ANALYTICAL SOLUTION

The analytical solution is developed based on Taylor's transform method. The displacement parameters, as analytical functions, may be expressed in terms of Taylor's series around *r=0,* based on a Kantorovich-type separation of variables.

$$u_0 = \sum_{k=0}^{N} U_k r^k e^{i\omega t}, \quad \psi^{(1)} = \sum_{k=0}^{N} \Psi_k^{(1)} r^k e^{i\omega t}, \quad \psi^{(2)} = \sum_{k=0}^{N} \Psi_k^{(2)} r^k e^{i\omega t}, \quad \psi^{(3)} = \sum_{k=0}^{N} \Psi_k^{(3)} r^k e^{i\omega t},$$
$$w = \sum_{k=0}^{N} W_k r^k e^{i\omega t} \tag{39}$$

By substituting Eq. (39) into the governing Eq. (36) and performing some manipulations, the transformed form of Eq. (36) may be written as:

$$\begin{aligned} \sum_{k=0}^{N} \Bigg\{ & \left(A^{(1)} + A^{(3)} + A^{(2)}\right)(k+1)(k+3)U_{k+2} + \left(B^{(1)} - \frac{h_2}{2}A^{(1)}\right)(k+1)(k+3)\Psi_{k+2}^{(1)} \\ & + \left(\frac{h_2}{2}A^{(1)} + B^{(2)} - \frac{h_2}{2}A^{(3)}\right)(k+1)(k+3)\Psi_{k+2}^{(2)} + \left(B^{(3)} + \frac{h_2}{2}A^{(3)}\right)(k+1)(k+3)\Psi_{k+2}^{(3)} \\ & + \left(I_0^{(1)} + I_0^{(2)} + I_0^{(3)}\right)\omega^2 U_k + \left(I_1^{(1)} - \frac{h_2}{2}I_0^{(1)}\right)\omega^2\Psi_k^{(1)} + \left(I_1^{(3)} + \frac{h_2}{2}I_0^{(3)}\right)\omega^2\Psi_k^{(3)} \\ & + \left[\frac{h_2}{2}\left(I_0^{(1)} - I_0^{(3)}\right) + I_1^{(2)}\right]\omega^2\Psi_k^{(2)} \Bigg\} r^k = 0 \end{aligned} \tag{40-a}$$

$$\sum_{k=0}^{N}\Bigg\{\left(B^{(1)}-\frac{h_2}{2}A^{(1)}\right)(k+3)(k+1)U_{k+2}+\left[\left(\frac{h_2}{2}\right)^2A^{(1)}-h_2B^{(1)}+D^{(1)}\right](k+3)(k+1)\Psi^{(1)}_{k+2}$$
$$+\frac{h_2}{2}\left(B^{(1)}-\frac{h_2}{2}A^{(1)}\right)(k+3)(k+1)\Psi^{(2)}_{k+2}-\kappa^{(1)}\overline{A}^{(1)}\left[\Psi^{(1)}_k+(L+1)W_{k+1}\right]+\Bigg[\ I^{(1)}_2-h_2I^{(1)}_1 \qquad (40\text{-b})$$
$$+\left(\frac{h_2}{2}\right)^2I^{(1)}_0\Bigg]\omega^2\Psi^{(1)}_k+\left(-\frac{h_2}{2}I^{(1)}_0+I^{(1)}_1\right)\omega^2U_k+\frac{h_2}{2}\left(I^{(1)}_1-\frac{h_2}{2}I^{(1)}_0\right)\omega^2\Psi^{(2)}_k\Bigg\}r^k=0$$

$$\sum_{k=0}^{N}\Bigg\{\left(\frac{h_2}{2}(A^{(1)}-A^{(3)})+B^{(2)}\right)(k+3)(k+1)U_{k+2}+\frac{h_2}{2}\left(B^{(1)}-\frac{h_2}{2}A^{(1)}\right)(k+3)(k+1)\Psi^{(1)}_{k+2}$$
$$+\left[\left(\frac{h_2}{2}\right)^2(A^{(1)}+A^{(3)})+D^{(2)}\right](k+3)(k+1)\Psi^{(2)}_{k+2}-\frac{h_2}{2}\left(B^{(3)}+\frac{h_2}{2}A^{(3)}\right)(k+3)(k+1)\Psi^{(3)}_{k+2}$$
$$-\kappa^{(2)}\overline{A}^{(2)}\left[\Psi^{(2)}_k+(k+1)W_{k+1}\right]+\left(\frac{h_2}{2}I^{(1)}_0+I^{(2)}_1-\frac{h_2}{2}I^{(3)}_0\right)\omega^2U_k+\frac{h_2}{2}\left(I^{(1)}_1-\frac{h_2}{2}I^{(1)}_0\right)\omega^2\Psi^{(1)}_k \qquad (40\text{-c})$$
$$+\left[\left(\frac{h_2}{2}\right)^2(I^{(1)}_0+I^{(3)}_0)+I^{(2)}_2\right]\omega^2\Psi^{(2)}_k-\frac{h_2}{2}\left(I^{(3)}_1+\frac{h_2}{2}I^{(3)}_0\right)\omega^2\Psi^{(3)}_k\Bigg\}r^k=0$$

$$\sum_{k=0}^{N}\Bigg\{\left(B^{(3)}+\frac{h_2}{2}A^{(3)}\right)(k+3)(k+1)U_{L+2}-\frac{h_2}{2}\left(\frac{h_2}{2}A^{(3)}+B^{(3)}\right)(k+3)(k+1)\Psi^{(2)}_{k+2}$$
$$-\kappa^{(3)}\overline{A}^{(3)}\left[\Psi^{(3)}_k+(k+1)W_{k+1}\right]\left(D^{(3)}+\frac{h_2}{2}B^{(3)}\right)(k+3)(k+1)\Psi_{k+2}$$
$$+\left[D^{(3)}+\frac{h_2}{2}\left(2B^{(3)}+\frac{h_2}{2}A^{(3)}\right)\right](k+3)(k+1)\Psi^{(3)}_{k+2}+\left(I^{(3)}_1+\frac{h_2}{2}I^{(3)}_0\right)\omega^2U_k \qquad (40\text{-d})$$
$$-\frac{h_2}{2}\left(\frac{h_2}{2}I^{(3)}_0+I^{(3)}_1\right)\omega^2\Psi^{(2)}_k+\left[I^{(3)}_2+h_2I^{(3)}_1+\left(\frac{h_2}{2}\right)^2I^{(3)}_0\right]\omega^2\Psi^{(3)}_k\Bigg\}r^k=0$$

$$\sum_{k=0}^{N}\Bigg\{\left(\kappa^{(1)}\overline{A}^{(1)}+\kappa^{(2)}\overline{A}^{(2)}+\kappa^{(3)}\overline{A}^{(3)}\right)(k+2)^2W_{k+2}+\kappa^{(1)}\overline{A}^{(1)}(k+2)\Psi^{(1)}_{k+1}+\kappa^{(2)}\overline{A}^{(2)}(k+2)\Psi^{(2)}_{k+1} \qquad (40\text{-e})$$
$$+\kappa^{(3)}\overline{A}^{(3)}(k+2)\Psi^{(3)}_{k+1}-(I^{(1)}_0+I^{(2)}_0+I^{(3)}_0)\omega^2W_k\Bigg\}r^k=0$$

By solving Eq. (40), an algebraic homogeneous system of equations including the unknown displacement parameters $U_{k+2}$, $\Psi^{(1)}_{k+2}$, $\Psi^{(2)}_{k+2}$, $\Psi^{(3)}_{k+2}$ and $W_{L+2}$ ($k=0,1,2,\ldots$) is obtained. The essential (geometric) boundary conditions must be incorporated to make this system of equations a deterministic one. Moreover, the regularity conditions at the center of the axisymmetric plate have to be imposed:

$$\begin{cases} u\big|_{r=0}=0 & \Rightarrow\ U_0=0 \\ \psi^{(1)}\big|_{r=0}=0 & \Rightarrow\ \Psi^{(1)}_0=0 \\ \psi^{(2)}\big|_{r=0}=0 & \Rightarrow\ \Psi^{(2)}_0=0 \\ \psi^{(3)}\big|_{r=0}=0 & \Rightarrow\ \Psi^{(3)}_0=0 \\ Q_r\big|_{r=0}=0 & \Rightarrow\ W_1=0 \end{cases} \tag{41}$$

By substituting Eq. (39) into the boundary conditions Eq. (37) the transformed form of Eq. (37) becomes:

$$\triangleright\ u=\sum_{L=0}^{N+2}U_k r^k=0,$$

*or*

$$\begin{aligned}\triangleright\ &\sum_{k=0}^{N+1}\Bigg\{\Big(A^{(1)}+A^{(2)}+A^{(3)}\Big)(k+1)U_{k+1}+\frac{1}{r}\Big(\tilde{A}^{(1)}+\tilde{A}^{(2)}+\tilde{A}^{(3)}\Big)U_k+\left(B^{(1)}-\frac{h_2}{2}A^{(1)}\right)(k+1)\Psi^{(1)}_{k+1}\\ &+\frac{1}{r}\left(\frac{h_2}{2}\tilde{A}^{(1)}+\tilde{B}^{(2)}-\frac{h_2}{2}\tilde{A}^{(3)}\right)\Psi^{(2)}_k+\left(\frac{h_2}{2}A^{(1)}+B^{(2)}-\frac{h_2}{2}A^{(3)}\right)(k+1)\Psi^{(2)}_{k+1}\\ &+\left(B^{(3)}+\frac{h_2}{2}A^{(3)}\right)(k+1)\Psi^{(3)}_{k+1}+\frac{1}{r}\left(\tilde{B}^{(3)}+\frac{h_2}{2}\tilde{A}^{(3)}\right)\Psi^{(3)}_k+\ \frac{1}{r}\left(\tilde{B}^{(1)}-\frac{h_2}{2}\tilde{A}^{(1)}\right)\Psi^{(1)}_k\Bigg\}r^k=0\end{aligned} \tag{42-a}$$

$$\triangleright\ \psi^{(1)}\Big|_{r=b}=\sum_{k=0}^{N+2}\Psi^{(1)}_k r^k=0,$$

or

$$\begin{aligned}\triangleright\ &\sum_{k=0}^{N+1}\Bigg\{\left(-\frac{h_2}{2}A^{(1)}+B^{(1)}\right)(k+1)\left(U_{k+1}-\frac{h_2}{2}\Psi^{(1)}_{k+1}+\frac{h_2}{2}\Psi^{(2)}_{k+1}\right)+\left(D^{(1)}-\frac{h_2}{2}B^{(1)}\right)(k+1)\Psi^{(1)}_{L+1}\\ &+\frac{1}{r}\left(\tilde{B}^{(1)}-\frac{h_2}{2}\tilde{A}^{(1)}\right)\left(U_k-\frac{h_2}{2}\Psi^{(1)}_k+\frac{h_2}{2}\Psi^{(2)}_k\right)+\frac{1}{r}\left(\tilde{D}^{(1)}-\frac{h_2}{2}\tilde{B}^{(1)}\right)\Psi^{(1)}_L\Bigg\}r^k=0\end{aligned} \tag{42-b}$$

$$\triangleright \quad \psi^{(2)}\Big|_{r=b} = \sum_{L=0}^{N+2} \Psi_k^{(2)} r^k = 0,$$

or

$$\begin{aligned}\triangleright \quad & \sum_{k=0}^{N+1}\Bigg\{\frac{h_2}{2}A^{(1)}(k+1)\left(U_{k+1}-\frac{h_2}{2}\Psi_{k+1}^{(1)}+\frac{h_2}{2}\Psi_{k+1}^{(2)}\right)+\frac{h_2}{2}\frac{1}{r}\tilde{A}^{(1)}\left(U_k-\frac{h_2}{2}\Psi_k^{(1)}+\frac{h_2}{2}\Psi_k^{(2)}\right)\\ & +\frac{h_2}{2}B^{(1)}(L+1)\Psi_{k+1}^{(1)}+\frac{h_2}{2}\frac{1}{r}\tilde{B}^{(1)}\Psi_k^{(1)}+B^{(2)}(k+1)U_{k+1}+\frac{1}{r}\tilde{B}^{(2)}U_k+D^{(2)}(k+1)\Psi_{k+1}^{(2)}\\ & +\frac{1}{r}\tilde{D}^{(2)}\Psi_k^{(2)}-\frac{h_2}{2}A^{(3)}(k+1)\left(U_{k+1}+\frac{h_2}{2}\Psi_{k+1}^{(3)}-\frac{h_2}{2}\Psi_{k+1}^{(2)}\right)-\frac{h_2}{2}B^{(3)}(k+1)\Psi_{k+1}^{(3)}\\ & -\frac{h_2}{2}\frac{1}{r}\tilde{A}^{(3)}\left(U_k+\frac{h_2}{2}\Psi_k^{(3)}-\frac{h_2}{2}\Psi_k^{(2)}\right)-\frac{h_2}{2}\tilde{B}^{(3)}\frac{1}{r}\Psi_k^{(3)}\Bigg\}r^k=0\end{aligned} \tag{42-c}$$

$$\triangleright \quad \psi^{(3)}\Big|_{r=b} = \sum_{L=0}^{N+2} \Psi_k^{(3)} r^k = 0,$$

or

$$\begin{aligned}\triangleright \quad & \sum_{k=0}^{N+1}\Bigg\{\left(B^{(3)}+\frac{h_2}{2}A^{(3)}\right)(k+1)\left(U_{k+1}+\frac{h_2}{2}\Psi_{k+1}^{(3)}-\frac{h_2}{2}\Psi_{k+1}^{(2)}\right)+\left(D^{(3)}+\frac{h_2}{2}B^{(3)}\right)(k+1)\Psi_{k+1}^{(3)}\\ & +\left(\tilde{B}^{(3)}+\frac{h_2}{2}\tilde{A}^{(3)}\right)\frac{1}{r}\left(U_k+\frac{h_2}{2}\Psi_k^{(3)}-\frac{h_2}{2}\Psi_k^{(2)}\right)+\left(\tilde{D}^{(3)}+\frac{h_2}{2}\tilde{B}^{(3)}\right)\frac{1}{r}\Psi_k^{(3)}\Bigg\}r^k=0\end{aligned} \tag{42-d}$$

$$\triangleright \quad w\big|_{r=b} = \sum_{k=0}^{N+1} W_k r^k = 0,$$

or

$$\begin{aligned}\triangleright \quad & \sum_{k=0}^{N+2}\Big[\left(\kappa^{(1)}\bar{A}^{(1)}+\kappa^{(2)}\bar{A}^{(2)}+\kappa^{(3)}\bar{A}^{(3)}\right)(k+1)W_{k+1}+\kappa^{(1)}\bar{A}^{(1)}\Psi_k^{(1)}+\kappa^{(2)}\bar{A}^{(2)}\Psi_k^{(2)}\\ & +\kappa^{(3)}\bar{A}^{(3)}\Psi_k^{(3)}\Big]r^k=0\end{aligned} \tag{42-e}$$

By substituting $U_k$, $\Psi_k^{(1)}$, $\Psi_k^{(2)}$, $\Psi_k^{(3)}$ and $W_k$ ($k=2,\ldots, N+2$) from Eq. (40) into Eq. (42), one obtains the following system of equations:

$$\begin{cases} \mathcal{S}_{11}^{(N)} U_1 + \mathcal{S}_{12}^{(N)} \Psi_1^{(1)} + \mathcal{S}_{13}^{(N)} \Psi_1^{(2)} + \mathcal{S}_{14}^{(N)} \Psi_1^{(3)} + \mathcal{S}_{15}^{(N)} W_0 = 0 \\ \mathcal{S}_{21}^{(N)} U_1 + \mathcal{S}_{22}^{(N)} \Psi_1^{(1)} + \mathcal{S}_{23}^{(N)} \Psi_1^{(2)} + \mathcal{S}_{24}^{(N)} \Psi_1^{(3)} + \mathcal{S}_{25}^{(N)} W_0 = 0 \\ \mathcal{S}_{31}^{(N)} U_1 + \mathcal{S}_{32}^{(N)} \Psi_1^{(1)} + \mathcal{S}_{33}^{(N)} \Psi_1^{(2)} + \mathcal{S}_{34}^{(N)} \Psi_1^{(3)} + \mathcal{S}_{35}^{(N)} W_0 = 0 \\ \mathcal{S}_{41}^{(N)} U_1 + \mathcal{S}_{42}^{(N)} \Psi_1^{(1)} + \mathcal{S}_{43}^{(N)} \Psi_1^{(2)} + \mathcal{S}_{44}^{(N)} \Psi_1^{(3)} + \mathcal{S}_{45}^{(N)} W_0 = 0 \\ \mathcal{S}_{51}^{(N)} U_1 + \mathcal{S}_{52}^{(N)} \Psi_1^{(1)} + \mathcal{S}_{53}^{(N)} \Psi_1^{(2)} + \mathcal{S}_{54}^{(N)} \Psi_1^{(3)} + \mathcal{S}_{55}^{(N)} W_0 = 0 \end{cases} \Rightarrow \quad \boldsymbol{\mathcal{S}}\,\boldsymbol{\Xi} = \mathbf{0} \tag{43}$$

$$\boldsymbol{\Xi}^T = \left\langle U_1 \quad \Psi_1^{(1)} \quad \Psi_1^{(2)} \quad \Psi_1^{(3)} \quad W_0 \right\rangle$$

Existence of a non-trivial solution for Eq. (43) requires that:

$$\left|\boldsymbol{\mathcal{S}}\right| = \mathbf{0} \tag{44}$$

## 6 RESULTS

In the present section, the proposed more general analytical shear correction factors and the elasticity-based formulations for the transverse shear stress are examined for the free vibration of sandwich circular plates with functionally graded layers. Although the presented expressions for the shear correction factor are mathematically proven, examination of the resulting enhancements in the results (in comparison with the available shear correction factors) cannot be accomplished for all types of analyses in a single paper. However, our previous experience has shown that effects of the shear correction factor in the free vibration analysis problems are more remarkable than those of cases where the external tractions act on the plate; because in the later cases, order of magnitude of the transverse shear stress is much smaller than order of magnitudes of the in-plane stresses. Since the functionally graded materials considered in the present section are mixtures of two of the steel, aluminium, and alumina materials, it is necessary to mention their materials properties:

Steel: $E = 210\,GPa,\ \nu = 0.3,\ \rho = 7850\,kg/m^3$

Aluminium: $E = 70\,GPa,\ \nu = 0.33,\ \rho = 2700\,kg/m^3$

Alumina: $E = 380\,GPa,\ \nu = 0.26,\ \rho = 3800\,kg/m^3$

Verification of the results and evaluation of the magnitude of the resulting enhancements are accomplished through comparing present results with results of the three-dimensional theory of elasticity extracted from ABAQUS finite element analysis code and results of employing the available commonly used correction factors.

### 6.1 Evaluation of the Employed Micromechanical Model for Variations of the Material Properties

It is known that the traditional linear rule of mixtures is an approximate model (Shariyat and Darabi, 2013; Shariyat, 2012b). To evaluate discrepancies of predictions of this model with respect to predictions of the more accurate Mori-Tanaka micromechanical-based model, a plate whose overall thickness is equal to $0.3m$ ($h_1=h_2=h_3=0.1m$) is considered. Two cases are considered and the through-thickness distributions of the elasticity modulus predicted by rule of mixtures and Mori-Tanaka model are compared in Fig. 2 and 3, respectively:

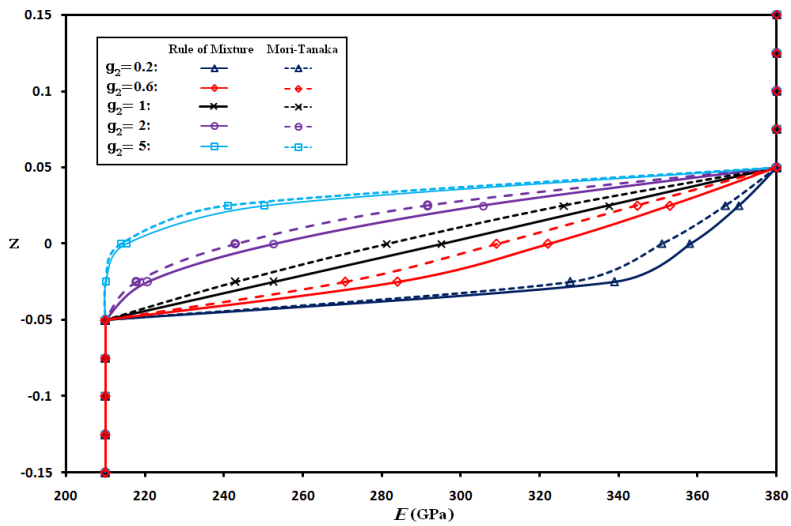


Figure 2: A comparison between predictions of the traditional rule of mixture and Mori-Tanaka model for trough-thickness variations of the elasticity modulus of the core of the sandwich plate, for various volume fraction indices.

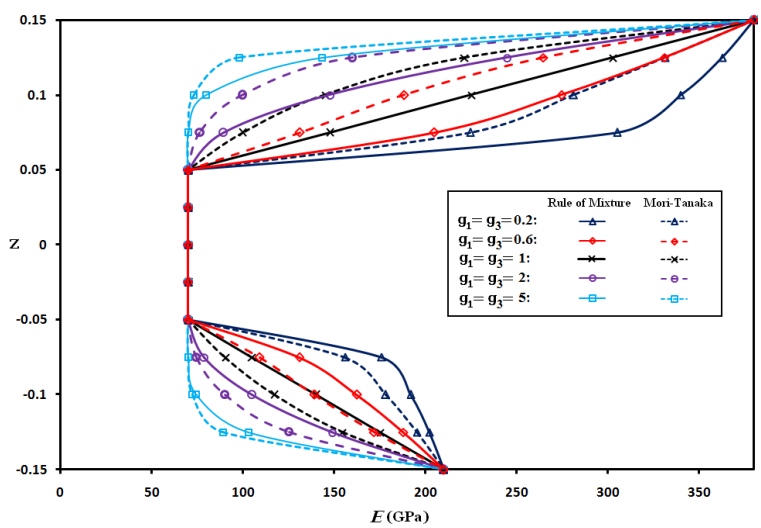


Figure 3: A comparison between predictions of the traditional rule of mixture and Mori-Tanaka model for trough-thickness variations of the elasticity modulus of the face sheets of the sandwich plate, for various volume fraction indices.

a) A plate with respectively alumina and steel top and bottom face sheets and a functionally graded core which is a transition medium (whose material properties vary from those of alumina to those of steel)
b) A plate with an aluminium core and functionally graded alumina/aluminium and aluminium/steel top and face sheets, respectively.

Comparing predictions of the two models reveals that the larger discrepancies occur at lower volume fraction indices. For the considered materials, the discrepancies are more remarkable when the face sheets are fabricated from functionally graded materials. Furthermore, for lower volume fraction indices, highest gradients occur in the neighborhood of the external surfaces of the face sheets and the upper surface of the core whereas the opposite is true for the higher volume fraction indices.

### 6.2 Verification of the Shear Correction Factor Expressions and Evaluation of the Enhancements

Since one of the inevitable sources of errors in the verification process is comparing results of various references that have used various formulations and different solution procedures. To prevent these common sources of errors, results of the present formulation are extracted based on the commonly used shear Mindlin correction factor for the circular plate ($\kappa=\pi^2/12$), our secondary suggestion for the sandwich plates ($\kappa=1$) with slightly softer cores, and the proposed analytical local correction factors. These results are compared with results of the three-dimensional theory of elasticity extracted from ABAQUS finite element analysis code. In this regard, results of the first three natural frequencies are compared for a relatively thick alumina/aluminium/steel circular sandwich plate with ($h_1/b=h_2/b=0.1$) in Table 1, for different edge conditions and core thickness to radius ratios ($h_2/b=h_c/b=0.1,\ 0.15,\ 0.2$). Relative deviations (differences) with respect to results of the 3D elasticity are also given in Table 1. Comparing these deviations shows that while our secondary suggestion for the shear correction factor leads to slightly more accurate results for the fundamental natural frequency, the generally accurate results belong to the developed analytical shear factor, especially for the higher (second and higher) natural frequencies. The unity correction factor can only be employed for cases wherein the core is either a transition medium or fabricated from a slightly softer material (as it is the case in the present example). In these cases, through-thickness distribution of the transverse shear resembles to some extent a rectangular (semi-uniform) or trapezoidal distribution. It may be readily deduced that Mindlin correction factor has led to significant errors in estimating contribution of the transverse shear stress. It is important to remind that since order of magnitude of the transverse shear stress is much lower than that of the bending stresses, the relevant strain energies and subsequently, relevant effects on the results are ignorable. Therefore, even ignorable differences in the results may reflect high effects of the shear correction factors. Since the ABAQUS results have been extracted based on Lagrangian ($C^0$-continuous) elements (3D quadratic eight-node axisymmetric CAX8R elements), they may encounter some minor inherent errors (this issue holds for all of the well-known commercial finite element analysis codes). Therefore, accuracy of the present shear correction factor

may actually be higher even for the fundamental natural frequency. As explained before, for calculation of the proposed shear factor, determination of the shear forces of the layers per unit layer is necessary. For the clamped plate, the mean relative difference with respect to results of the 3D elasticity is respectively 1.45, 3.58, and 0.87 for $\kappa=1$, $\kappa=\pi^2/12$, and the present analytical correction factor (based on the relevant vibration mode shape). For the simply supported and free edge conditions, these relative differences are (0.84, 2.78, and 0.82) and (0.98, 1.78, and 0.87), respectively. Therefore, the shear correction factors that have mainly been proposed for the single-layer plates are not adequate for the multilayer plates. The main reason is that the assumption of the equivalent single-layer theories that states that the entire layers of the plate section rotate identically is not accurate and in many cases may be erroneous. In many cases, direction of rotation of the core may even be opposite to and quite different from that of the face sheets (Alipour and Shariyat, 2014b).

| Edge Condition | Approach | $h_c/b=0.1$ | | | $h_c/b=0.15$ | | | $h_c/b=0.2$ | | |
|---|---|---|---|---|---|---|---|---|---|---|
| | | $\omega_1$ | $\omega_2$ | $\omega_3$ | $\omega_1$ | $\omega_2$ | $\omega_3$ | $\omega_1$ | $\omega_2$ | $\omega_3$ |
| Clamped | 3D (ABAQUS) | 768.58 | 2118.3 | 3639.4 | 818.26 | 2164.4 | 3615.3 | 857.3 | 2202 | 3536.5 |
| | Present $\varkappa=1$ | 770.431 | 2140.9 | 3730.8 | 820.04 | 2193.8 | 3704.2 | 859.43 | 2240.4 | 3648.8 |
| | Difference (%) | 0.24 | 1.07 | 2.51 | 0.22 | 1.36 | 2.46 | 0.25 | 1.74 | 3.17 |
| | Present $\varkappa=\pi^2/12$ | 738.09 | 2026.1 | 3539.2 | 779.42 | 2067.1 | 3550.4 | 812.20 | 2104.2 | 3550.6 |
| | Difference (%) | 3.97 | 4.35 | 2.75 | 4.75 | 4.5 | 1.8 | 5.26 | 4.44 | 0.4 |
| | Present, analytical | 764.8 | 2113.4 | 3675.2 | 814.56 | 2168.9 | 3675.8 | 853.74 | 2213.3 | 3635.9 |
| | Difference (%) | 0.49 | 0.23 | 0.98 | 0.45 | 0.21 | 1.67 | 0.42 | 0.51 | 2.81 |
| Simply supported | 3D (ABAQUS) | 462.85 | 1904.9 | 2195 | 522.48 | 1983 | 2128.5 | 574.04 | 2042 | 2073.2 |
| | Present $\varkappa=1$ | 461.83 | 1910.7 | 2219.5 | 520.49 | 1991.8 | 2163.3 | 571.07 | 2056 | 2120.4 |
| | Difference (%) | 0.22 | 0.31 | 1.12 | 0.38 | 0.44 | 1.63 | 0.52 | 0.69 | 2.28 |
| | Present $\varkappa=\pi^2/12$ | 453.51 | 1819.9 | 2203.6 | 508.04 | 1884.7 | 2144.2 | 554.55 | 1938.1 | 2097.7 |
| | Difference (%) | 2.02 | 4.46 | 0.39 | 2.76 | 4.96 | 0.74 | 3.4 | 5.09 | 1.18 |
| | Present, analytical | 460.7 | 1894.2 | 2216.8 | 519.25 | 1977 | 2161.9 | 569.81 | 2042.4 | 2118.6 |
| | Difference (%) | 0.46 | 0.56 | 0.99 | 0.62 | 0.3 | 1.57 | 0.74 | 0.02 | 2.19 |
| Free | 3D (ABAQUS) | 791.79 | 2132.9 | 2421.9 | 880.56 | 2099.6 | 2476.2 | 955.15 | 2061.4 | 2519.4 |
| | Present $\varkappa=1$ | 791.85 | 2149.7 | 2447.2 | 880.12 | 2125.5 | 2514.5 | 954.42 | 2098 | 2576.6 |
| | Difference (%) | 0.01 | 0.79 | 1.05 | 0.05 | 1.23 | 1.55 | 0.08 | 1.78 | 2.27 |
| | Present $\varkappa=\pi^2/12$ | 777.72 | 2100.7 | 2374.9 | 860.09 | 2084.3 | 2414.3 | 928.96 | 2060.2 | 2459.0 |
| | Difference (%) | 1.78 | 1.51 | 1.94 | 2.32 | 0.73 | 2.5 | 2.74 | 0.06 | 2.4 |
| | Present, analytical | 789.8 | 2142.3 | 2432.8 | 878.05 | 2120.5 | 2498.5 | 952.33 | 2094.9 | 2561.6 |
| | Difference (%) | 0.25 | 0.44 | 0.45 | 0.28 | 1 | 0.9 | 0.3 | 1.63 | 1.68 |

Table 1: A comparison among values of the first three natural frequencies (in Hz) of a relatively thick alumina/aluminium/steel sandwich plate predicted based on employing various correction factors and the 3D elasticity, for various core thickness ratios and different edge conditions ($h_1/b=h_2/b=0.1$).

### 6.3 Sandwich Plates with Functionally Graded Face Sheets and Different Edge Conditions

As a next stage, it is assumed that the face sheets are fabricated from functionally graded materials ($g=1$) to constitute an alumina-aluminium/aluminium/aluminium-steel sandwich plate. In this regard, results of the present formulation (up to the fifth natural frequency) are compared with results of $\kappa=1$ and results of the 3D elasticity in Tables 2 and 3, for the clamped, and simply supported and free edge conditions, respectively. Results are calculated for various core thickness ratios.

| Natural frequency (Hz) | $h_c/b$ | $h_1/b=h_2/b=0.075$ | | | | | $h_1/b=h_2/b=0.1$ | | | | |
|---|---|---|---|---|---|---|---|---|---|---|---|
| | | 3D (ABAQUS) | Present $\kappa=1$ | Difference (%) | Present, analytical | Difference (%) | 3D (ABAQUS) | Present $\kappa=1$ | Difference (%) | Present, analytical | Difference (%) |
| $\omega_1$ | 0.1 | 695.12 | 707.02 | 1.71 | 694.62 | 0.07 | 775.55 | 797.33 | 2.81 | 776.83 | 0.16 |
| | 0.15 | 763.16 | 773.86 | 1.4 | 758.06 | 0.67 | 828.43 | 848.32 | 2.4 | 824.71 | 0.45 |
| | 0.2 | 816.65 | 826.26 | 1.18 | 802.91 | 1.68 | 870.2 | 888.48 | 2.1 | 865.61 | 0.53 |
| $\omega_2$ | 0.1 | 1983.1 | 2047 | 3.22 | 1981.5 | 0.08 | 2126.5 | 2222.9 | 4.53 | 2128 | 0.07 |
| | 0.15 | 2082.6 | 2138.3 | 2.67 | 2067 | 0.75 | 2191.7 | 2277.8 | 3.93 | 2186 | 0.26 |
| | 0.2 | 2157.1 | 2207.6 | 2.34 | 2116.9 | 1.86 | 2242.5 | 2322.7 | 3.58 | 2236.4 | 0.27 |
| $\omega_3$ | 0.1 | 3462.4 | 3599.4 | 3.96 | 3458.9 | 0.1 | 3635.3 | 3764.4 | 3.55 | 3635.8 | 0.01 |
| | 0.15 | 3554.2 | 3651.3 | 2.73 | 3533 | 0.6 | 3595 | 3701.5 | 2.96 | 3645.7 | 1.41 |
| | 0.2 | 3539.3 | 3631.3 | 2.6 | 3550.5 | 0.32 | 3497.3 | 3643.3 | 4.17 | 3614.7 | 3.36 |
| $\omega_4$ | 0.1 | 3763.1 | 3842.5 | 2.11 | 3823.4 | 1.6 | 3730.8 | 3929.7 | 5.33 | 3835.7 | 2.81 |
| | 0.15 | 3653.1 | 3787.3 | 3.67 | 3741.5 | 2.42 | 3695.7 | 3943.5 | 6.7 | 3794.9 | 2.68 |
| | 0.2 | 3639 | 3808 | 4.64 | 3689.8 | 1.4 | 3717.5 | 3971.4 | 6.83 | 3808.9 | 2.46 |
| $\omega_5$ | 0.1 | 4986.7 | 5287.3 | 6.03 | 5033.6 | 0.94 | 5139.3 | 5611.6 | 9.19 | 5272.4 | 2.59 |
| | 0.15 | 5036.8 | 5355.5 | 6.33 | 5103.2 | 1.32 | 5100 | 5620.3 | 10.2 | 5329.8 | 4.51 |
| | 0.2 | 5056.7 | 5406.1 | 6.91 | 5115.9 | 1.17 | 5050 | 5593 | 10.8 | 5348.4 | 5.91 |

Table 2: Relative differences of predictions made for the first five natural frequencies of a clamped sandwich plate with functionally graded face sheets (alumina-aluminium/aluminum/aluminium-steel sandwich plate), with respect to the three-dimensional theory of elasticity ($g=1$).

While results of Table 2 are extracted for $h_1/b=h_3/b=0.075,\ 0.1$, results of Table 3 are computed for $h_1/b=h_3/b=0.05$. Results of Tables 2 and 3 reveal that while our two suggestions for the shear correction factor may lead to relatively accurate results, results of the analytical shear correction are generally more accurate, especially for the higher modes. The mean relative differences with

respect to results of the 3D elasticity that are summarized in Table 4 confirm this conclusion. Furthermore, for thinner plates and lower vibration modes, usage of the correction factor does not seem to be a necessity if the core is fabricated from a slightly softer material. Because in such cases, through-thickness distribution of the transverse shear stress resembles a rectangular (uniform) distribution rather than a parabolic or a skewed parabolic one. However, if severe differences exist between elastic moduli of the layers, the unity correction factor cannot be employed.

| Natural frequency (Hz) | $h_c / b$ | Simply Supported | | | | | Free | | | | |
|---|---|---|---|---|---|---|---|---|---|---|---|
| | | 3D (ABAQUS) | Present $\varkappa=1$ | Difference (%) | Present, analytical | Difference (%) | 3D (ABAQUS) | Present $\varkappa=1$ | Difference (%) | Present, analytical | Difference (%) |
| $\omega_1$ | 0.1 | 324.22 | 324.65 | 0.13 | 323.76 | 0.14 | 571 | 572.48 | 0.26 | 570.65 | 0.06 |
| | 0.15 | 387.37 | 387.4 | 0.01 | 386.28 | 0.28 | 673.16 | 674.23 | 0.16 | 672.05 | 0.17 |
| | 0.2 | 443.5 | 443.05 | 0.1 | 441.72 | 0.4 | 760.83 | 761.47 | 0.08 | 758.86 | 0.26 |
| $\omega_2$ | 0.1 | 1556.4 | 1570.2 | 0.89 | 1550.9 | 0.35 | 1899.1 | 1915.9 | 0.88 | 1895.8 | 0.18 |
| | 0.15 | 1737 | 1746.2 | 0.53 | 1725.9 | 0.64 | 1974.8 | 1989.3 | 0.73 | 1984 | 0.47 |
| | 0.2 | 1873.8 | 1879.4 | 0.3 | 1859.1 | 0.79 | 1952.5 | 1972.8 | 1.04 | 1970.5 | 0.92 |
| $\omega_3$ | 0.1 | 2048.3 | 2059.1 | 0.53 | 2058.1 | 0.48 | 2082.3 | 2095.4 | 0.63 | 2090.4 | 0.39 |
| | 0.15 | 1997.6 | 2013.3 | 0.78 | 2012.3 | 0.74 | 2159.8 | 2175.4 | 0.72 | 2155 | 0.22 |
| | 0.2 | 1958.5 | 1980 | 1.1 | 1978.9 | 1.05 | 2291.3 | 2304.3 | 0.57 | 2279.9 | 0.5 |
| $\omega_4$ | 0.1 | 3058.3 | 3111.2 | 1.73 | 3047.0 | 0.37 | 3467.4 | 3530.1 | 1.81 | 3460.5 | 0.2 |
| | 0.15 | 3273 | 3316.8 | 1.34 | 3255.5 | 0.53 | 3671.9 | 3727.8 | 1.52 | 3661.7 | 0.28 |
| | 0.2 | 3421.8 | 3462.9 | 1.2 | 3405.1 | 0.49 | 3786 | 3843.5 | 1.52 | 3780.7 | 0.14 |
| $\omega_5$ | 0.1 | 4607.8 | 4736.6 | 2.79 | 4605.2 | 0.06 | 4948.8 | 5088.6 | 2.82 | 4976.6 | 0.56 |
| | 0.15 | 4804.8 | 4931.6 | 2.64 | 4811.9 | 0.15 | 4885.9 | 5102.5 | 4.43 | 5048.8 | 3.33 |
| | 0.2 | 4697.1 | 5042.1 | 7.34 | 4956.0 | 5.51 | 4699.4 | 5042.2 | 7.29 | 5009.7 | 6.6 |

Table 3: Relative differences of predictions made for the first five natural frequencies of alumina-aluminium/aluminum/aluminium-steel sandwich plates with simply supported or free edges, with respect to the three-dimensional theory of elasticity ($g=1$, $h_1/b=h_2/b=0.05$).

| Edge condition | Present $\varkappa=1$ | Present, analytical |
|---|---|---|
| Clamped ($h_1/b=h_2/b=0.075$) | 3.43 | 1 |
| Clamped ($h_1/b=h_2/b=0.1$) | 5.27 | 1.83 |
| Simply supported | 1.43 | 0.8 |
| Free | 1.63 | 0.95 |

**Table 4:** Relative differences of the results of the zigzag theory for different shear correction factors of a sandwich plate having functionally graded face sheets, with respect to the three-dimensional theory of elasticity.

Some of the vibration modes are related to the in-plane deformations. Therefore, plotting the vibration modes may help in discussion of the nature of the resulting enhancements. Lateral deflections of the plate in the first five vibration modes are shown in Fig. 4 for the mid-plane of the clamped sandwich plates with ($h_1/b=h_2/b=0.075$ and $h_2/b=0.1$). Moreover, 3D plots of the in-plane displacement of the plate are plotted in Fig. 5 for the same vibration shape modes. Comparing Fig. 4 and 5 reveals that the fourth mode is an in-plane vibration mode. The remaining four modes are transverse ones. The fourth mode is the first in-plane vibration mode. While the natural frequencies of the transverse displacement increase with the thickness of the plate, the first natural frequency of the in-plane displacements has decreased by increasing the thickness of the sandwich plate.

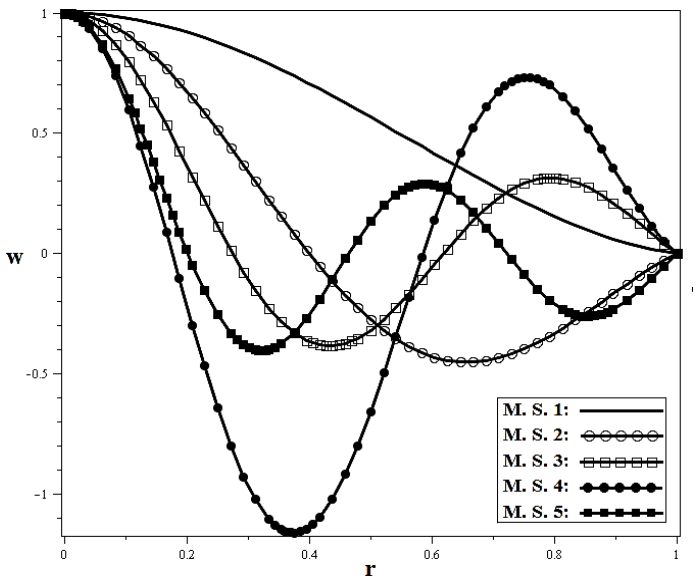


Figure 4: Lateral deflections of the clamped sandwich plate with functionally graded face sheets, in the first five vibration modes.

Similarly, the vibration modes are studied for sandwich plates with functionally graded face sheets and simply supported or free edge conditions. The modal transverse and in-plane displacements of the sandwich plate are plotted in Fig. 6 and 7 for the simply supported edge condition ($h_1/b=h_2/b=0.05$ and $h_2/b=0.1$) and in Figs. 8 and 9 for the plate with a free edge ($h_1/b=h_2/b=0.05$ and $h_2/b=0.2$). According to Figs. 6 and 7, the third mode is associated with the in-plane displacements and the remaining modes are associated with the lateral deflections. As before, the natural frequencies related to resonances associated with the lateral deflections increase with thickness of the plate whereas those associated with the in-plane displacements decrease by increasing the thickness of the sandwich plate. For the sandwich plate with a free edge, according to Figs. 8 and 9, the second and fifth vibration modes are associated with the in-plane modal displacements and the remaining modes are associated with the lateral deflections of the plate.

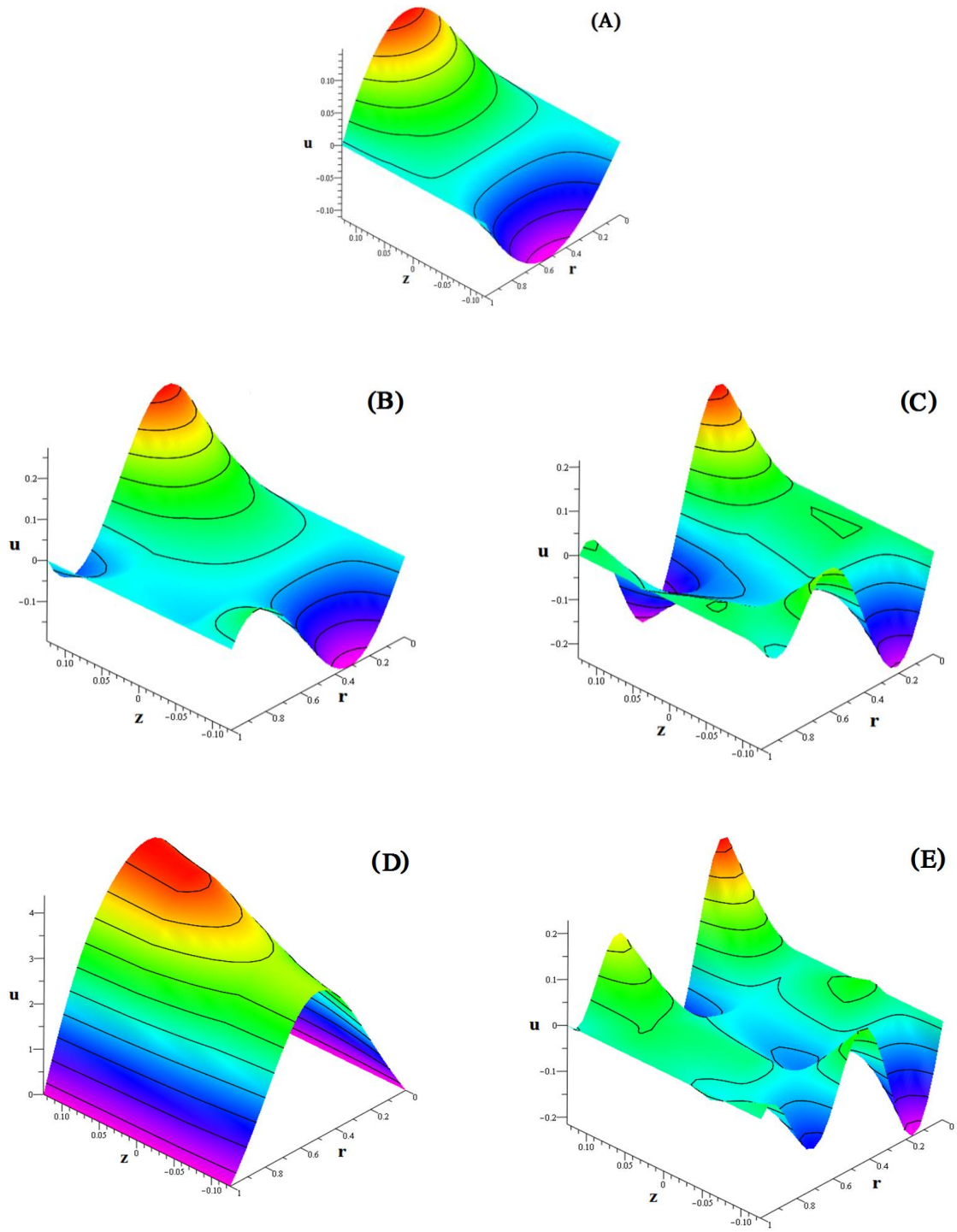


Figure 5: In-plane displacements of the clamped sandwich plate with functionally graded face sheets in the first five vibration modes, respectively.

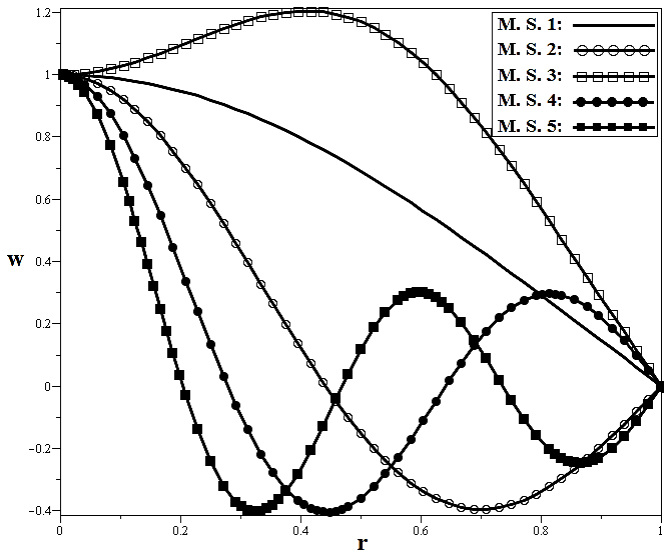


Figure 6: Lateral deflections of the simply supported sandwich plate with functionally graded face sheets, in the first five vibration modes.

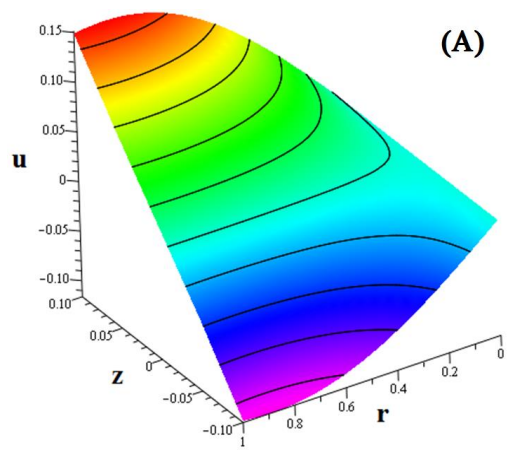

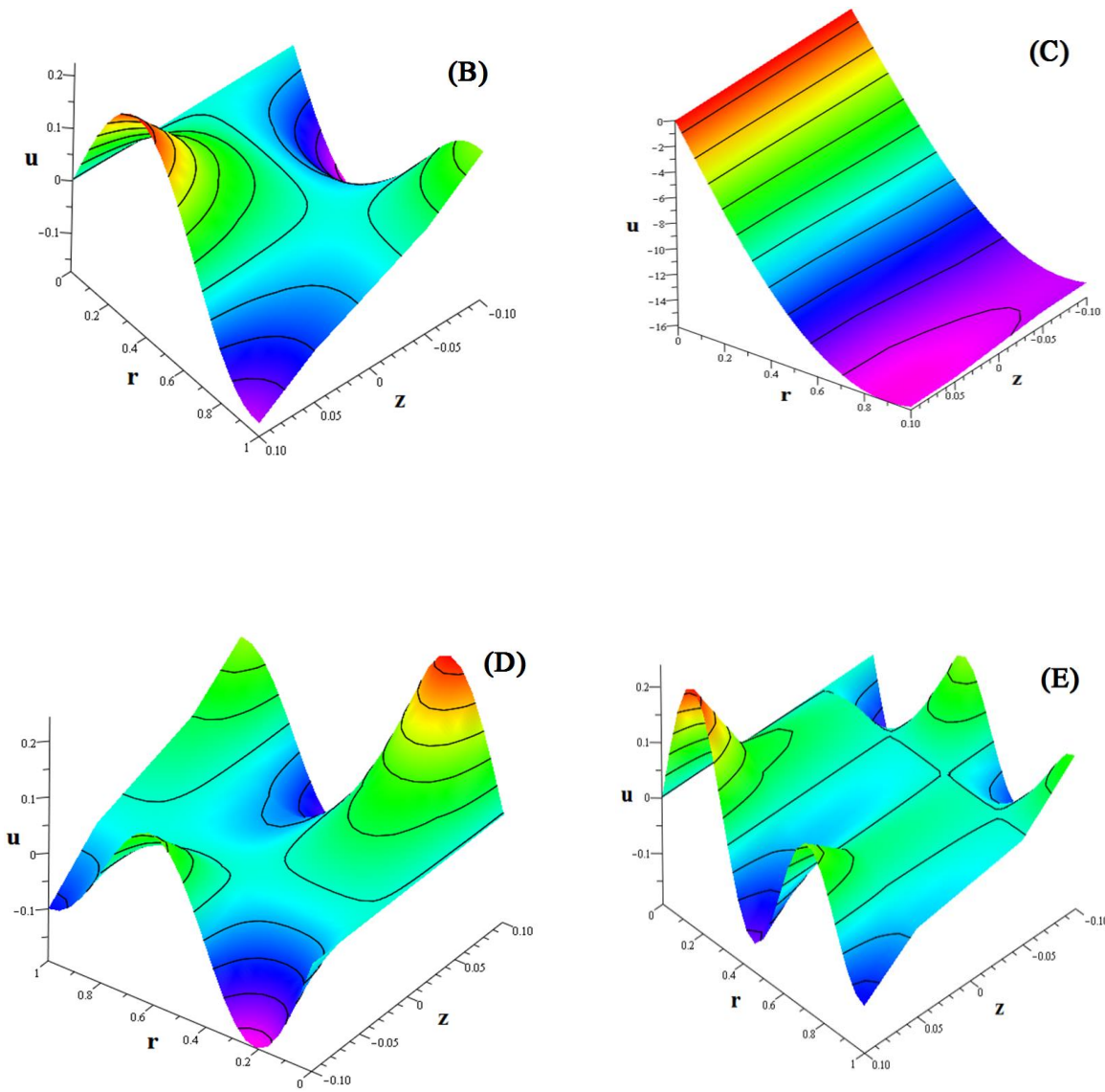


Figure 7: In-plane displacements of the simply supported sandwich plate with functionally graded face sheets in the first five vibration modes, respectively.

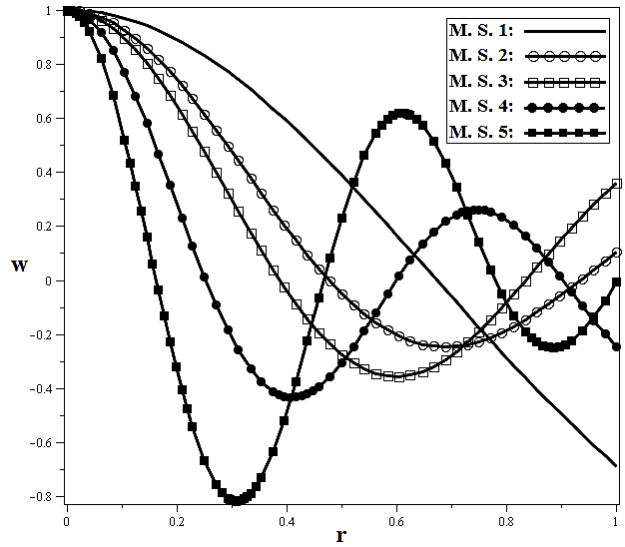


Figure 8: Lateral deflections of the sandwich plate with functionally graded face sheets and a free edge, in the first five vibration modes.

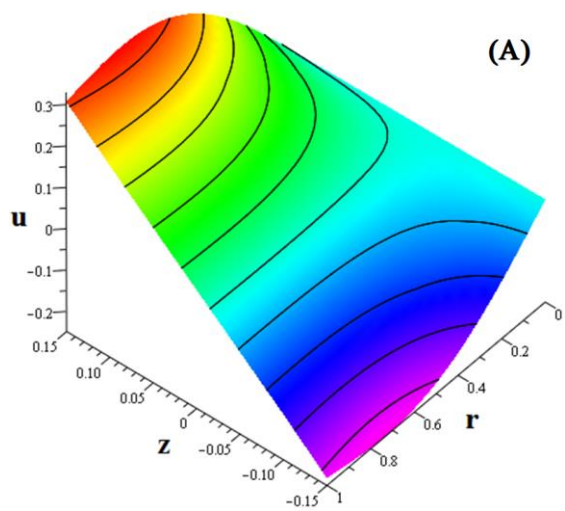

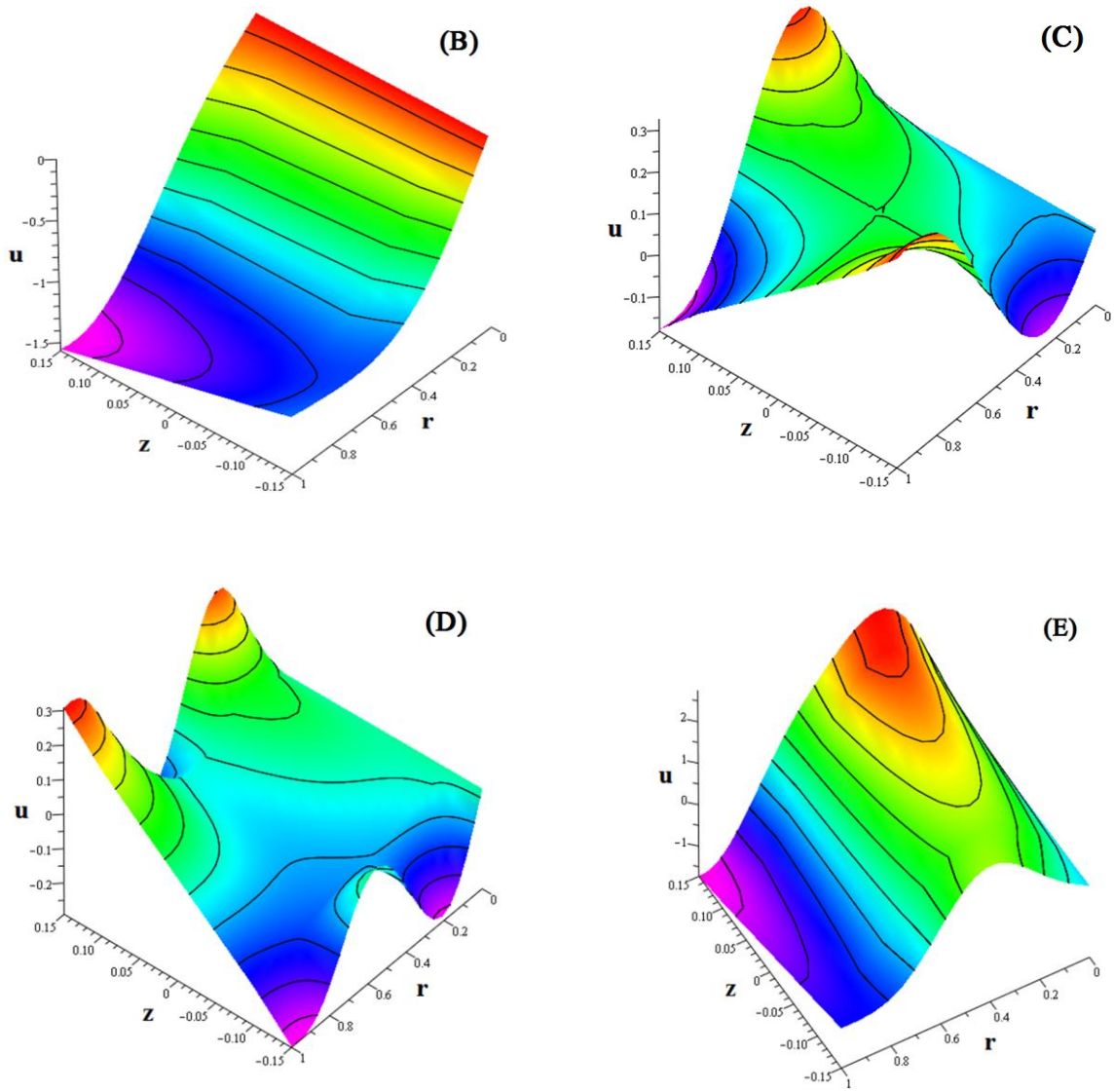


Figure 9: In-plane displacements of the sandwich plate with functionally graded face sheets and a free edge, in the first five vibration modes, respectively.

## 7 CONCLUSIONS

Two suggestions are given in the present paper for shear correction factors that are especially suitable for the more general case of a sandwich plate with functionally graded layers, subjected to normal and shear tractions. The first suggestion that is suitable for lower vibration modes of thin plates with a slightly softer core is using a unity correction factor. Since in these cases, the resulting transverse distribution of the shear stress may resemble a semi-uniform or trapezoidal one in these cases. The more reliable shear correction factor is an analytical and layerwise one that have been

derived based on the equivalence of the elasticity-based and the constitutive-equations-based strain energies of the transverse shear stresses. The available shear correction factors have mainly been proposed for rectangular plates with zero shear tractions and isotropic homogenous materials. In derivation of these shear factors, it was assumed that local rotations of the layers are identical; an assumption that does not hold for the sandwich plates wherein direction of rotation of the core may even be opposite those of the face sheets. Although the proposed analytical shear correction factors are very general, they are evaluated for the modal analysis wherein effects of the shear correction are more remarkable than those of the stress analyses. It is the first time that concept of the local shear correction factor is introduced. To present more accurate results, the Mori-Tanaka micromechanical-based material properties model is used instead of the traditional rule of mixtures. The governing equations are solved using the analytical Taylor transform technique. Detailed discussion of the comparative example presented in the results section reveals that significant enhancements may occur through using the proposed analytical shear correction factors.

## References

Alipour, M.M., Shariyat, M., (2010). Stress analysis of two-directional FGM moderately thick constrained circular plates with non-uniform load and substrate stiffness distributions, Journal of Solid Mechanics 2: 316-331.

Alipour, M.M., Shariyat, M., (2011a). Semi-analytical buckling analysis of heterogeneous variable thickness viscoelastic circular plates on elastic foundations, Mechanics Research Communications 38: 594-601.

Alipour, M.M., Shariyat, M., (2011b). A power series solution for free vibration of variable thickness Mindlin circular plates with two-directional material heterogeneity and elastic foundations, Journal of Solid Mechanics 3: 183-197.

Alipour, M.M., Shariyat, M., (2012). An elasticity-equilibrium-based zigzag theory for axisymmetric bending and stress analysis of the functionally graded circular sandwich plates, using a Maclaurin-type series solution, European Journal of Mechanics - A/Solids 34: 78-101.

Alipour, M.M., Shariyat, (2013). M., A semi-analytical solution for buckling analysis of variable thickness two-directional functionally graded circular plates with non-uniform elastic foundations, ASCE Journal of Engineering Mechanics 139: 664-676.

Alipour, M.M., Shariyat, M., (2014a). An analytical global–local Taylor transformation-based vibration solution for annular FGM sandwich plates supported by nonuniform elastic foundations, Archive of Civil and Mechanical Engineering 14: 6–24.

Alipour, M.M., Shariyat, M., (2014b). Analytical stress analysis of annular FGM sandwich plates with non-uniform shear and normal tractions, employing a zigzag-elasticity plate theory. Aerospace Science and Technology 32: 235 – 259.

Alipour, M.M., Shariyat, M., Shaban, M., (2010). A semi-analytical solution for free vibration of variable thickness two-directional-functionally graded plates on elastic foundations, International Journal of Mechanics and Materials in Design 6: 293-304.

Cowper, G.R., (1966). The shear coefficient in Timoshenko beam theory, ASME Journal of Applied Mechanics 33: 335-340.

Chróścielewski, J., Pietraszkiewicz, W., Witkowski, W., (2010). On shear correction factors in the non-linear theory of elastic shells, International Journal of Solids and Structures 47: 3537–3545.

Ebrahimi, F., Rastgoo, A., Atai, A.A., (2009). A theoretical analysis of smart moderately thick shear deformable annular functionally graded plate, European Journal of Mechanics - A/Solids 28: 962–973.

Efraim, E., Eisenberger, M., (2007), Exact vibration analysis of variable thickness thick annular isotropic and FGM plates, Journal of Sound and Vibration 299: 720–738.

Fares, M.E.,. Elmarghany, M.Kh., (2008). A refined zigzag nonlinear first-order shear deformation theory of composite laminated plates, Composite Structures 82: 71-83.

Gruttmann, F., Wagner, W., (2001). Shear correction factors in Timoshenko's beam theory for arbitrary shaped cross-sections, Computational Mechanics 27: 199–207.

Hutchinson, J.R., (1981). Transverse vibration of beams, exact versus approximate solutions, Journal of Applied Mechanics 48: 923–928.

Hutchinson, J.R., (2001). Shear coefficients for Timoshenko beam theory, Journal of Applied Mechanics 68: 87–92.

Kaneko, T., (1975). On Timoshenko's correction for shear in vibrating beams, Journal of Physics D 8: 1927–1936.

Mantari, J.L., Oktem, A.S., Guedes Soares, C., (2011). Static and dynamic analysis of laminated composite and sandwich plates and shells by using a new higher-order shear deformation theory, Composite Structure 94: 37–49.

Menaa, R., Tounsi, A., Mouaici, F., Mechab, I., Zidi, M., Adda Bedia, E.A., (2012). Analytical solutions for static shear correction factor of functionally graded rectangular beams, Mechanics of Advanced Materials and Structures 19: 641-652.

Mindlin, R.D., (1951). Influence of rotatory inertia and shear in flexural motions of isotropic elastic plates, ASME Journal of Applied Mechanics 18: 1031–1036.

Murthy, A.V.K., (1970). Vibration of short beams, AIAA Journal 8: 34-38.

Nguyen, T.-K., Sab, K., Bonnet, G., (2008). First-order shear deformation plate models for functionally graded materials, Composite Structures 83: 25–36.

Pai, P.F., Schulz, M.J., (1999). Shear correction factors and an energy consistent beam theory, International Journal of Solids and Structures 36: 1523-1540.

Pandit, M.K., Sheikh, A.H., Singh, B.N., (2008). An improved higher order zigzag theory for the static analysis of laminated sandwich plate with soft core, Finite Elements in Analysis and Design 44: 602-610.

Rebello, C.A., Bbert, C.W., Gordaninejad, F., (1983). Vibration of bimodular sandwich beams with thick facings: a new theory and experimental results, Journal of Sound and Vibration 90: 381-397.

Reddy, J.N., Wang, C.M., Kitipornchai, S., (1999). Axisymmetric bending of functionally graded circular and annular plates, European Journal of Mechanics A/Solids 18: 185-199.

Reddy, J.N., (2005). Theory and analysis of elastic plates and shells, 2nd ed., CRC Press (Boca Raton).

Shariyat, M., (2009a). Dynamic buckling of imperfect laminated plates with piezoelectric sensors and actuators subjected to thermo-electro-mechanical loadings, considering the temperature-dependency of the material properties, Composite Structures 88:228–39.

Shariyat, M., (2009). Vibration and dynamic buckling control of imperfect hybrid FGM plates with temperature-dependent material properties subjected to thermo-electro-mechanical loading conditions, Composite Structures 88: 240–52.

Shariyat, M., (2010). Non-linear dynamic thermo-mechanical buckling analysis of the imperfect sandwich plates based on a generalized three-dimensional high-order global–local plate theory, Composite Structures 92: 72-85.

Shariyat, M., Alipour, M.M., (2010). A differential transform approach for modal analysis of variable thickness two-directional FGM circular plates on elastic foundations, ISME 11: 15-38.

Shariyat, M., (2012a). A general nonlinear global-local theory for bending and buckling analyses of imperfect cylindrical laminated and sandwich shells under thermomechanical loads, Meccanica 47: 301-319.

Shariyat, M., (2012b). Nonlinear transient stress and wave propagation analyses of the FGM thick cylinders, employing a unified generalized thermoelasticity theory, International Journal of Mechanical Sciences 65: 24-37.

Shariyat, M., Alipour, M.M., (2013a). A power series solution for vibration and complex modal stress analyses of variable thickness viscoelastic two-directional FGM circular plates on elastic foundations, Applied Mathematical Modelling 37: 3063-3076.

Shariyat, M., Alipour, M.M., (2013b) Semi-analytical consistent zigzag-elasticity formulations with implicit layer-wise shear correction factors for dynamic stress analysis of sandwich circular plates with FGM layers, Composites Part B 49: 43-64.

Shariyat, M., Darabi, E., (2013). A variational iteration solution for elastic-plastic impact of polymer/clay nanocomposite plates with or without global lateral deflection, employing an enhanced contact law, International Journal of Mechanical Sciences 67: 14-27.

Shariyat, M., Jafari, R., (2013). A micromechanical approach for semi-analytical low-velocity impact analysis of a bidirectional functionally graded circular plate resting on an elastic foundation, Meccanica 48: 2127–2148.

Sofiyev, A.H., (2014). Large-amplitude vibration of non-homogeneous orthotropic composite truncated conical shell, Composites Part B: Engineering 61: 365 – 374.

Stephen, N.G., (1997). Mindlin plate theory: best shear coefficient and higher spectra validity, Journal of Sound and Vibration 202: 539–53.

Timoshenko, S.P., (1922). On the transverse vibrations of bars of uniform cross section, Philosophical Magazine 43: 125–131.

Wittrick, W.H., (1987). Analytical, three dimensional elasticity solution to some plates problems, and some observations on Mindlin's plate theory, International Journal of Solids and Structures 23: 441-464.